Creating Porous Hydrogel Scaffolds using Templating Alginate Microspheres

Matt J. Fiedler

A thesis

submitted in partial fulfillment of the

requirements for the degree of

Master of Science in Mechanical Engineering

University of Washington

2012

Amy Q. Shen, Chair

Jaehyun Chung

Buddy Ratner

Program Authorized to Offer Degree:

Department of Mechanical Engineering

University of Washington

Abstract

Creating Porous Hydrogel Scaffolds using Templating Alginate Microspheres

Matt J. Fiedler

Chairs of Supervisory Committee:

Associate Professor: Amy Shen
Department of Mechanical Engineering

Some of the greatest areas of advancement in the medical field are currently in areas such as tissue engineering, implant fixation, and drug delivery techniques involving the use of scaffolds. A scaffold is an artificial three dimensional porous structure that can support tissue formation within the body. For scaffolds to be most successful, they should have monodisperse pores, interconnected pores, a highly ordered microstructure, and controllable pore size. To accomplish this task, templating alginate microspheres were created using microfluidics and then packed into a microchannel. A UV polymerizable hydrogel was then flowed over the alginate spheres and polymerized. After the polymerization, the alginate spheres were removed using EDTA so that a porous hydrogel scaffold can be obtained. This process was successful as a proof of concept, but there are still details that need to be improved.

Table of Contents

List of Figures

List of Tables

Acknowledgements

I would like to thank Professor Amy Shen for all of her support, knowledge, and guidance throughout this project. I would also like to thank Dr. Perry Chung and Jess Stockham for their valuable insight into many of the difficult problems encountered during the project. The University of Washington Nanotechnology User Facility has also been an extremely helpful through providing the necessary tools, facilities and staff needed for the success of this work. My friends and family also deserve a great deal of thanks for their continual support.

Chapter 1 Introduction

Some of the greatest areas of advancement in the medical field are currently in areas such as tissue engineering, implant fixation, and drug delivery techniques. For each of these areas, one of the most intriguing methods for advancement is through using three dimensional porous scaffolds due to their ability to mimic native extracellular matrices [1]. Scaffolds with good biocompatibility as well as biodegradability have minimal impact on the body [2]. The cost of these scaffolds is also often very low, making porous scaffolds an incredibly viable option for the future in design of medical implants [3].

In order to minimize the impact on the body, it is important to mimic living tissues. To do this, scaffolds are often made of hydrogels because they offer unique mechanical and structural properties as well as high water content, making them very similar to living tissue [4]. It has also been found that scaffolds are much more effective when pore monodispersity, interconnectivity, and appropriate pore size are present so that cellular attachment and proliferation can occur [5]. In a study by Professor Buddy Ratner's group, it was found that when interconnectivity was present in the scaffold, a 30-40 micron pore size showed the greatest healing and tissue generation [6].

In the past, scaffolds have been made using many different methods such as salt leaching, phase separation, gas foaming, and fiber meshes [7]. With all of these methods it has been very difficult to make the pores a specific size and to ensure monodispersity [8, 9]. An additional problem is that the interconnectivity of the pores has been difficult to attain [8, 9]. These problems have caused scaffolds to be much less successful than their potential suggests. In response to these issues, Ratner's group used templating PMMA microspheres to create monodisperse and interconnected porous hydrogel scaffolds [10]. This was done through packing PMMA microspheres in a microchannel and sintering the microspheres in order to create interconnects. A UV polymerizable hydrogel was then flowed over the spheres and polymerized using a UV lamp to create the scaffold. The PMMA microspheres were then dissolved out using acetone, leaving the hydrogel scaffold with interconnected pores. This method worked extremely well to make the porous hydrogel scaffolds, but using a toxic solvent to dissolve out the PMMA microspheres makes the scaffold undesirable for biological applications.

To solve the problems of high polydispersity, a lack of interconnected pores, and the use of toxic chemicals, microfluidics will be used to make a biocompatible porous hydrogel scaffold in this thesis. To accomplish this goal, the following objectives must be met.

Objectives

I. Droplet microfluidics will be used to create alginate drops that are monodisperse between 30-40 microns. To do this, a microfluidic T-junction will be used where 2% alginate is the dispersed phase, and soybean oil with 0.5% Span 85 is the continuous phase.
II. After the alginate drops have been created, they will then be polymerized using calcium chloride. To do this, the calcium chloride and alginate must coalesce and mix so that the alginate drops will become hard microspheres. A novel microfluidic design must be used to cause the calcium chloride and alginate to coalesce while still holding the original spherical shape and the same diameter.
III. The polymerized alginate microspheres will then be packed into a microfluidic channel. Since it is important that the porous hydrogel scaffold has pores arranged in a hexagonal close packed plane, sonication must take place as the microspheres are entering the channel. This will cause the microspheres to go to their thermodynamic minimum which will correspond to the correct packing structure.
IV. After the packing has occurred, a UV polymerizable hydrogel will be flowed over the alginate microspheres. The microspheres should be soaked in the hydrogel for a specified amount of time so that the alginate microspheres will soften slightly and cause interconnects to form between the microspheres.
V. The microfluidic device containing the microspheres and hydrogel needs to then be placed under a UV light so the hydrogel will polymerize.
VI. The polymerized hydrogel and alginate microspheres then needs to be removed from the microchannel and soaked in Ethylenediaminetetraacetic acid (EDTA) to dissolve out the alginate. For optimum dissolving to take place, sonication will be done on the scaffold while it is in the EDTA, so that the alginate will be agitated and removed more easily.
VII. A cross section of the porous hydrogel scaffold will be cut and imaged using Scanning Electron Microscopy. This will allow the pores, interconnectivity, and packing structure to be analyzed to see whether the desired objectives have been met.

Chapter 2 Literature Review

2.1 Scaffolds

2.1.1 Uses and Characteristics

A scaffold is an artificial structure that allows three-dimensional tissue formation to take place after cells have been implanted within the structure. Within the medical field and specifically tissue engineering, scaffolds are extremely promising for the development of biological substitutes that regenerate, replace, maintain, or improve the function of damaged tissue[11]. Each of these applications relies on the growth and formation of a desired tissue to take place. In order for the tissue growth to occur, the growth must be done in a scaffold [12]. Often the scaffolds are porous and three dimensional so that nutrients can be transferred more efficiently and so that the exposed surface area of the scaffold is maximized. In many of these applications, the scaffold essentially serves as a synthetic extra cellular matrix which organizes cells into a three dimensional architecture that presents stimuli to direct the growth and formation of the desired tissue. Many times this occurs by a scaffold occupying the space of natural tissue and then providing the framework so that the desired tissue can be regenerated[13]. The scaffolds show major promises in the areas of bioactive molecular delivery, cell/tissue delivery, and space filling agents.

Bioactive molecular delivery uses scaffolds to deliver bioactive molecules and encapsulate secretory cells to specific areas of the body. Currently most drug delivery occurs through oral or intravenous delivery rather than with a scaffold at a specific location. Consequently, a much larger amount of the drug must be used since the application of the drug is not localized. Not only is this extremely costly and wasteful, but it can also have serious side effects. The drug that is applied may be beneficial for a particular tissue, but harmful or even toxic for another type of tissue. Through using a scaffold and localizing drug delivery, this is no longer a problem [13].

Cell/tissue delivery is another area that scaffolds show a great deal of promise due to their ability to host cells to adhere, differentiate, and proliferate. Through changing the mechanical properties of the scaffold, different chemical signals and growth factors can be applied to the cells, giving large control over the tissue developed. This method has often been used for engineering tissues such as bone, cartilage, muscle, fat, and neurons [13]. Additionally,

scaffolds have been used as space filling agents. For this application, the scaffold must provide adhesion and function as a bioadhesive. These have been used to treat urinary incontinence, for plastic and reconstructive surgeries, and for biological adhesives for soft tissues [13].

Several key characteristics should be present in the scaffold for their effective functionality in the applications described above. One of the most important aspects of the scaffold is that it must be both biocompatible and biodegradable [14]. It is also extremely important for the scaffold to have an ordered microstructure and uniform pore size for several reasons. If the scaffold is being used for drug delivery, a uniform pore distribution will ensure that the chemicals are distributed homogeneously [12]. It is also important because when the scaffold is used for cell growth, uniform microstructure is necessary for the cells to have consistent growth conditions. If they do not, there will be cellular inconsistencies within the three dimensional system[11]. This will then also cause inhomogeneous cell distribution which leads to non-uniform degradation of scaffold materials [14]. Another important characteristic of the scaffold is that the pores be interconnected to encourage cell growth through increased flow transport of nutrients as well as metabolic waste [15]. Additionally, the size of the pores is extremely important. In a study performed by Ratner et al, scaffolds with different pore sizes were implanted into mice. To analyze which scaffold caused the greatest growth, blood vessel density was measured and the results were compiled into Figure 2.1 [16].

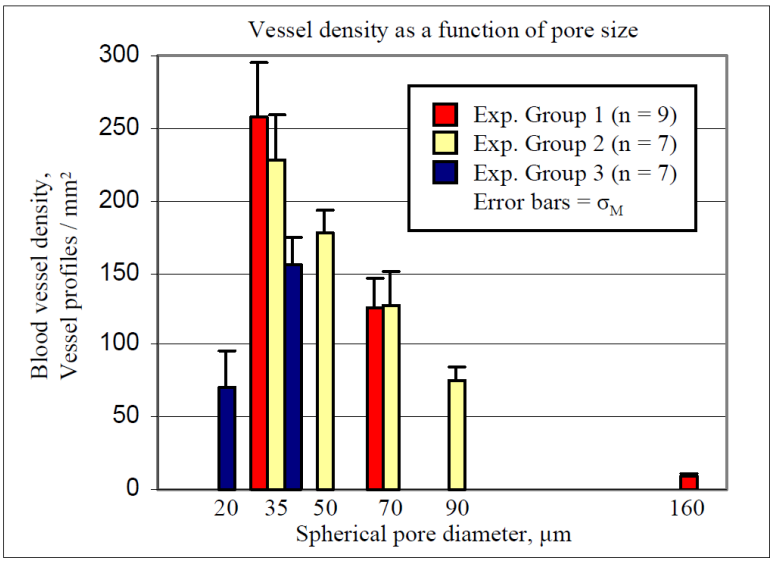

Figure 2.1: A 35 µm pore size has the greatest regeneration properties [16]

From the figure it can be seen that the greatest blood vessel density occurs with a spherical pore diameter of 35 µm. The optimal pore size is not the same for all applications, but

regardless of the application it is important to have control over the pore size so that the optimum pore size can be reached.

2.1.2 Different fabrication techniques for porous scaffolds

In 2010 Hwang et al. created porous hydrogel scaffolds for general tissue engineering applications [14]. The specific focus was on creating a scaffold that had good porosity to enable rapid nutrient and oxygen transfer. The technique used templating gelatin spheres in an alginate hydrogel.

The scaffold was constructed by first creating gelatin emulsions in oil using the emulsification method. The emulsification method is performed through mixing two immiscible fluids together in a controlled manner to form drops of the aqueous phase in the oil phase. This method is very quick and simple, but the resulting drops generally have a high polydispersity. During the emulsification process, the liquids were kept at a high temperature, but after the emulsification process was complete, the mixture of oil and gelatin was cooled to cause the gelatin drops to harden and form microspheres. Since the emulsification method gives high polydispersity, a sieving process was performed to select the spheres that were 150-300 um in diameter. These microspheres were then placed in a 2% alginate solution and mixed so that the microspheres were evenly distributed within the alginate solution. The full process used is shown in Figure 2.2.

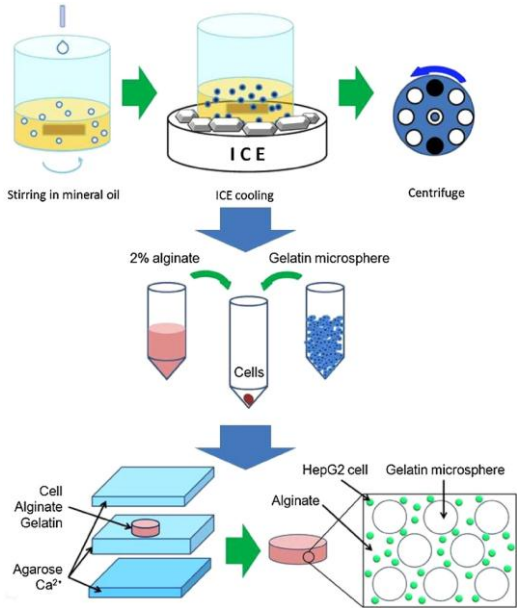

Figure 2.2: The process used by Hwang et al. to create porous scaffolds [14]

The alginate and gelatin microsphere mixture was subsequently placed in a solid mold made of agarose and calcium chloride. Through the diffusion of calcium chloride into Alginate, polymerization occurred. At this point the temperature was raised back up so that the gelatin microspheres melted and were removed leaving a porous scaffold. Using this method the scaffold shown in Figure 2.3 was created.

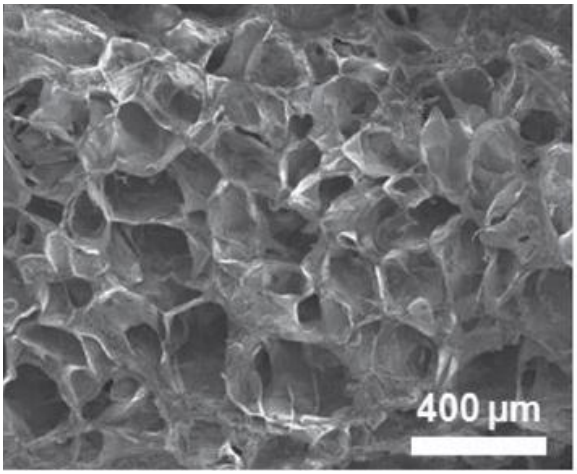

Figure 2.3: Hwang et al created this scaffold using the method described above [14]

From this figure it can be seen that a porous scaffold was created. However, polydispersity is high within the scaffold since the emulsification method was used to create the templating microspheres. There is also not an ordered packing structure present in the scaffold, since there was no control of the packing that took place. The lack of packing control resulted in inconsistent interconnects as well.

Testouri et al. also created porous hydrogel scaffolds for similar applications, but by using a different type of hydrogel, and a different fabrication method [17]. These scaffolds were made using Chitosan, which is a biopolymer that works extremely well for scaffolds since it is biodegradable and biocompatible. The method that was used to create the scaffold used a gas foaming method rather than solid spheres as templates.

The gas foaming method used by Testouri created 1.25 mm diameter bubbles in chitosan using a millifluidic T-junction device. The flow rates of the air and chitosan were applied using high precision flow rate syringe pumps, which led to precise control over the size and frequency of the bubble production. After the bubbles were created, glyoxal was added into the channel to begin the polymerization of the chitosan. As the polymerization took place, the

bubbles were flowed into a bath where they self-organized into a close packed structure before completely solidifying. For this method to be successful, extensive rheological tests were used to study the polymerization time of the chitosan and glyoxal reaction. The reaction time was extremely important because if the polymerization time was too short, the bubbles would not have time to pack into the correct structure, but if the polymerization time was too long, bubble coalescence would transpire. The method used to create these scaffolds is shown in Figure 2.4.

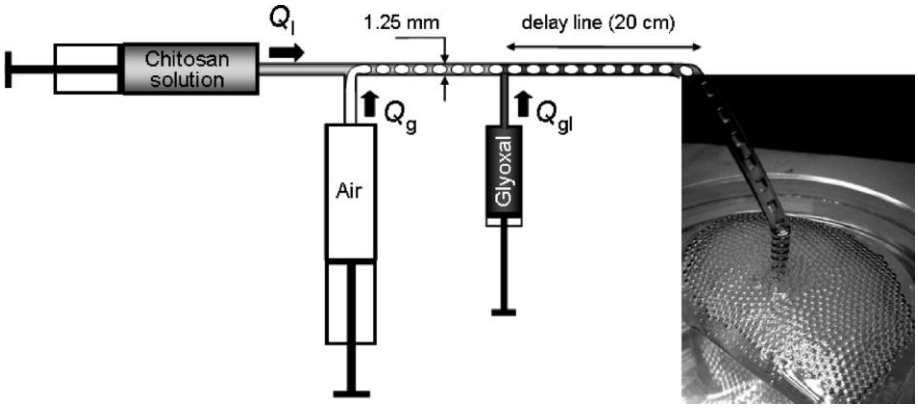

Figure 2.4: The process used by Testouri et al. to create porous scaffolds [17]

Constructing the scaffolds using this method has many benefits such as high monodispersity of the pores, and a very good packing structure as shown in Figure 2.5.

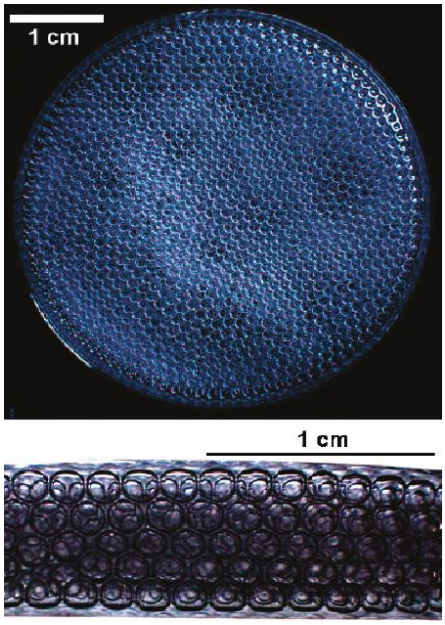

Figure 2.5: Testouri et al created this close packed array of bubbles using the gas bubble method [17]

Although the monodispersity is high in this scaffold, the interconnectedness of the pores is limited since it is individual bubbles that form the scaffold. There is also difficulty in using this same method to create scaffolds made with different types of hydrogel materials due to the fact that the polymerization that occurs in other fluids is often not as easy to control as it is with chitosan. This scaffold is made with milli size pores rather than micron size pores which limits the number of potential applications as well.

To address the issues such as high polydispersity, a lack of packing structure, and limited interconnectivity of pores, Linnes et al. created a scaffold using templating PMMA microbeads [10]. To do this, 50 micron PMMA beads were placed into a microchannel and sonicated in a sonication bath until close packing was achieved. The microchannel filled with PMMA spheres was next heated until the PMMA spheres sintered into one single piece. Doing this caused the microbeads to have interconnects that had a diameter 50% of the bead diameter. At this point a polyHEMA hydrogel was flowed over the top of the packed microspheres and polymerized using a UV lamp. The interconnected PMMA microbeads were then dissolved out of the scaffold using acetone as the solvent. The resulting scaffold is shown in Figure 2.6.

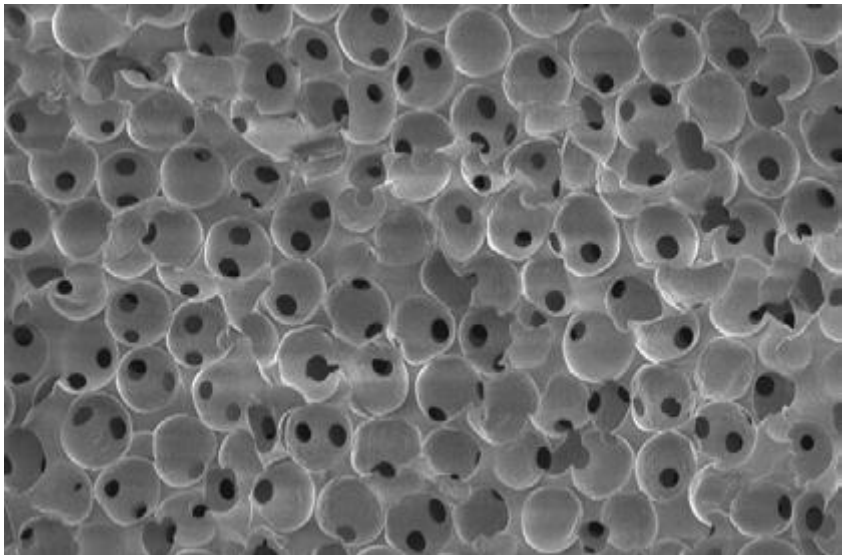

Figure 2.6: Linnes et al created this porous scaffold using templating PMMA microspheres [10]

As can be seen from Figure 2.6, this method for creating scaffolds has extremely monodisperse pores, monodisperse interconnects, and a highly ordered packing structure. These specific characteristics have been achieved much better by this scaffold fabrication method than nearly all other types of scaffolds. The drawback to using this method, is that enzymes cannot be

placed within the scaffold and survive being exposed to acetone when the PMMA spheres are rinsed out. This greatly limits the applications for which the scaffold can be applied.

2.2 Micron size droplet production

Recently droplet microfluidics has gained a great deal of attention due to its many applications involving reaction [18], mixing [19], emulsions [20], biomedicine [21], and material synthesis[22]. Droplet microfluidics is excellent for these applications due to the precise control over size and frequency of droplet production. Most droplet microfluidics takes place inside a microfluidic device, and uses either a T-junction, flow focusing, or co-flowing geometry for droplet production. These different types of flow geometry are shown in Figure 2.7 [23].

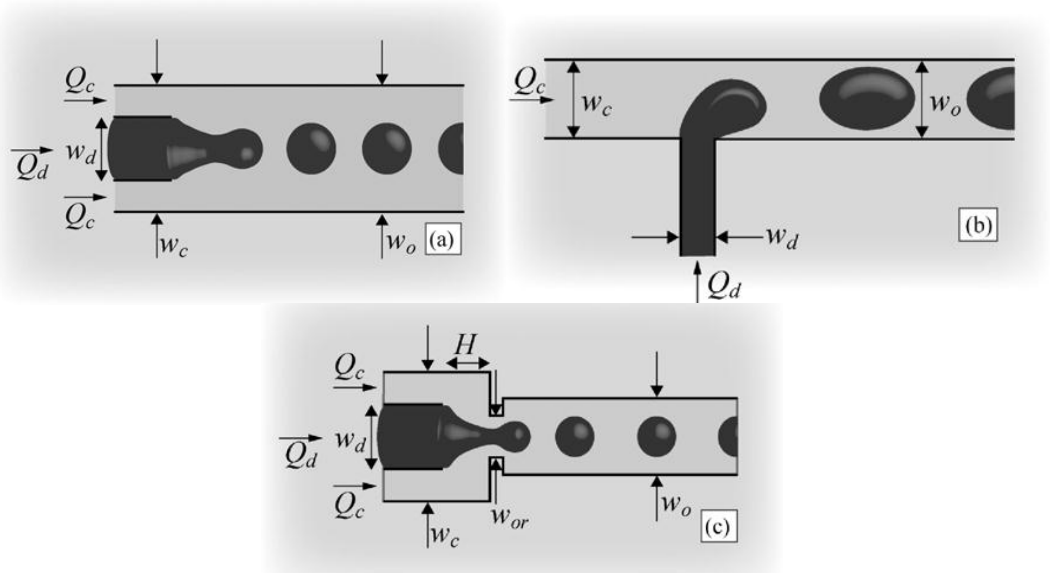

Figure 2.7: Schematic examples of (a) co-flow, (b) T-junction, and (c) flow focusing microfluidic devices [23]

All three of these flow geometries work with the same general droplet breakoff principle. Each has a dispersed phase, which is the liquid that the drops are made out of, and a continuous phase which is the liquid that surrounds the droplet. The continuous and dispersed phase flow rates are controlled separately using either a constant pressure or constant volumetric flow rate. For each of these methods, the dispersed phase protrudes into the channel where the continuous phase is flowing and gradually fills up a larger portion of the flow area. As this happens, the pressure increases behind the dispersed phase which gradually deforms the interface until droplet breakoff occurs. In general, the droplet breakup can be characterized by the competition between local fluid stresses acting to deform the liquid interface and capillary pressure acting to resist deformation [23].

There are several important dimensionless numbers to consider when using droplet microfluidics. Since the droplet breakup process is dependent on the balance between viscous and interfacial stresses, the capillary number shown in equation 2.1 is extremely important to consider[24].

2.1 $$Ca = \frac{\mu U}{\sigma}$$

Here μ is the zero shear viscosity of the disperse fluid, U is the fluid velocity, and σ is the interfacial tension between the two immiscible fluids. This essentially shows the ratio of viscous stresses to interfacial stresses. For an individual geometry, the capillary number can often predict whether droplet breakoff will occur. Since there are many types of flow geometry used, the exact capillary number to give optimal droplet breakoff varies greatly. Generally it has been reported that capillary numbers between 10^{-3} and 1 give the best droplet break off, but it is necessary to use experimental procedures for a given system to find the appropriate capillary number for optimum droplet breakoff [23].

The flow rate ratio is another vital parameter to consider when performing droplet microfluidics as shown in equation 2.2.

2.2 $$\varphi = \frac{Q_d}{Q_c}$$

Here the numerator refers to the flow rate of the dispersed phase while the denominator is the flow rate of the continuous phase. The flow rate ratio is generally the largest contributor to the size of the droplet that is produced. The relationship between the flow rate and the droplet size is again very dependent on the geometry of the system. For a T-junction in a narrow channel, the equation 2.3 generally describes the relationship well [25].

2.3 $$\frac{L}{w} = \varepsilon + \delta\varphi$$

Here L is the length of the drop that is produced, w is the width of the droplet, ε and δ are fitting parameters, and φ is the flow rate ratio. Equation 2.3 shows that the flow rate ratio versus droplet size is a linear relationship. Grastenecki et al. also found that the relationship between the flow rate and droplet size is linear as shown in Figure 2.8 [26].

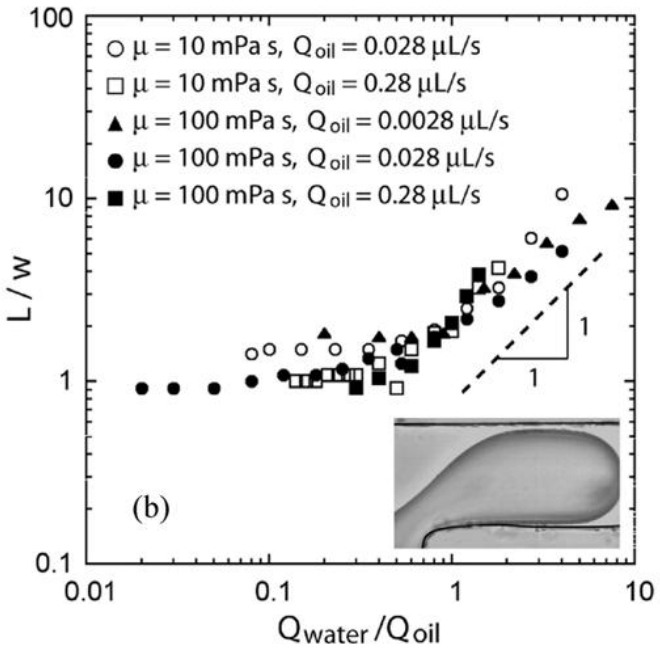

Figure 2.8: Study by Grastenecki et al showing that the size of drops is a function of the flow rate ratio [26]

Depending on the geometry and fluid properties the relationship will vary, but within confined flow droplet production, a linear relationship can be used in order to characterize the droplet size.

Although the capillary number and flow rate ratio are generally the most influential non dimensional numbers to consider, the viscosity ratio should also be mentioned.

$$\lambda = \frac{\mu_d}{\mu_c} \tag{2.4}$$

Here the numerator is the viscosity of the dispersed phase, and the denominator is the continuous phase. Generally if the ratio is extremely large or extremely small, droplet production will be difficult to obtain.

2.3 Alginate polymerization

Polymerization is a process involving monomer molecules reacting with another chemical to form polymer chains, often resulting in a solid. This process occurs when alginate is in the presence of calcium ions as shown in the chemical reaction in equation 2.5 [27] .

$$2\ Na\ alginate\ (l) + CaCl_2(l) \rightarrow Ca\ alginate\ (s) + 2\ NaCl(l) \tag{2.5}$$

One way to supply the calcium ions to the alginate for polymerization is by mixing alginate with calcium chloride. When this happens, solid calcium alginate is formed. For this application it is desired to polymerize the monodisperse alginate drops so that solid spheres are formed. This can be done through merging the alginate drops with calcium chloride. Since the alginate and calcium chloride are both immiscible in the continuous phase, coalescence of two fluids is not a trivial matter.

Huang et al. reported a very simple method for coalescence of two fluids in 2007 [28]. In this study alginate drops were created using a flow focusing device before being flowed through a tube and dropped directly into a bath of calcium chloride where polymerization occurred. The basic method used is shown in Figure 2.9.

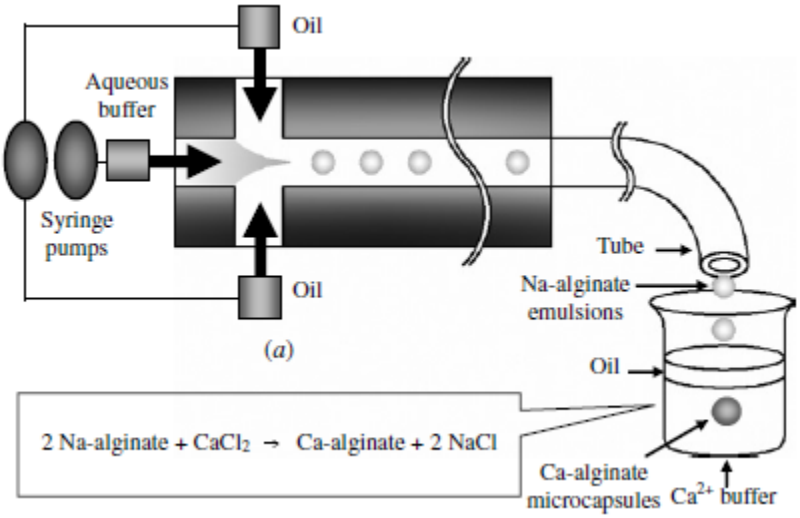

Figure 2.9: Method used by Huang et al to polymerize alginate drops [28]

Using this system it is reported that extremely monodisperse polymerized drops are created, and that the drops are nearly instantly polymerized when exposed to the 20% calcium chloride in the bath. Since the system only consists of creating droplets and flowing the droplets into the calcium chloride, the process is extremely simple. However, one of the problems that can easily occur with this system is that the alginate drops will coalesce with other alginate drops before exiting the tube and contacting the calcium chloride. When this happens, the polydispersity increases dramatically. The drops also have the opportunity to coalesce when in the top layer of oil before entering into the calcium chloride. These problems can be eliminated when conditions are optimal, but if there are any slight variations or inconsistencies in the pumps or other aspects of the flow, alginate drop coalescence can quickly occur.

Other droplet coalescence methods have also been used as shown by Liu et al. Liu et al. used one flow focusing device to create alginate drops, and another flow focusing device to create calcium chloride drops. These drops then met at a junction and coalesced in a series of chambers as shown in Figure 2.10 [29].

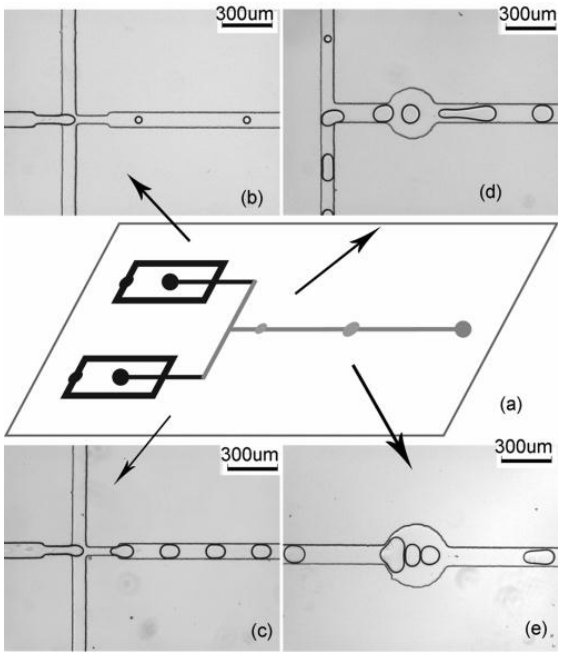

Figure 2.10: Method used by Liu et al to polymerize alginate drops [29]

In the device shown in the figure, the drops meet at a junction after exiting the flow focusing devices, but merge in the circular chambers following the junction, rather than at the junction. When a drop enters one of the circular chambers it slows down dramatically allowing the droplet behind it to draw nearer to it so that coalescence will occur.

The biggest advantage with this device is that it is possible to finely control the size of both the alginate and calcium chloride drops that are created since flow focusing devices are used. As the flow rates are changed to control the droplet size, the droplet frequency changes as well. For correct coalescence to occur, however, both flow focusing devices need to have similar frequencies. If this does not occur, non-polymerized alginate drops will coalesce and the polydispersity will increase greatly. In order for the system to work as desired, a great deal of fine tuning is necessary. The system is also very susceptible to small flow perturbations which can cause large problems.

Jin et. al caused alginate and calcium chloride microspheres to coalesce using a different approach [30]. In this study, a double T-junction was used as shown in Figure 2.11.

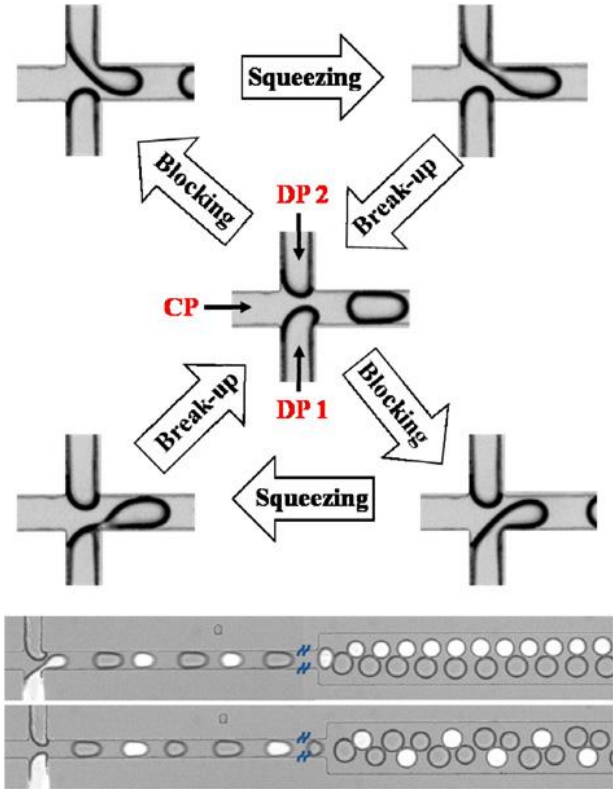

Figure 2.11: Method used by Jin et al to polymerize alginate drops [30]

In this system the continuous phase enters from the left most channel, while the alginate enters from the top and calcium chloride enters from bottom channel before flowing to the right. The droplet breakup occurs the same way as with a typical T-junction, except that after breakoff has occurred with one of the dispersed phases, the other dispersed phase will naturally enter the channel. Breakoff will then occur with that phase, which leads to drops alternating naturally as shown in the lower portion of Figure 2.11. In order for coalescence to occur, a velocity difference needs to be present between the two different types of drops which may exist due to differences in drop size or viscosity.

This is a novel design that has been successful in creating alternating drops with low polydispersity. Given a long enough channel, the alginate drops have a high rate of coalescence with the calcium chloride drops. Since the system of alternating drops happens naturally, this system does not have the same problem as the double flow focusing design described used by Liu et al. Although the alternating drops occur naturally, the coalescence of drops is not always

consistent with the system if there small perturbations take place. The size of the drops that are produced relies heavily on the geometry, so it is difficult to make polymerized spheres that are much bigger or smaller than the width of the channel.

2.4 Packing spheres

The monodisperse drops that are produced and polymerized are used as templating spheres for the porous hydrogel scaffold that is being created. To produce porous hydrogel scaffolds with an ordered structure, it is necessary to pack the microspheres into a close packed structure. Packing the microspheres into this close packed structure has been explored by researchers in the past for a variety of different applications.

Park and Xia obtained a close packed structure of beads ranging from the sizes of 50 nm to 1 μm for the purpose of fabricating optical sensors [31]. The method that was used is shown in Figure 2.12.

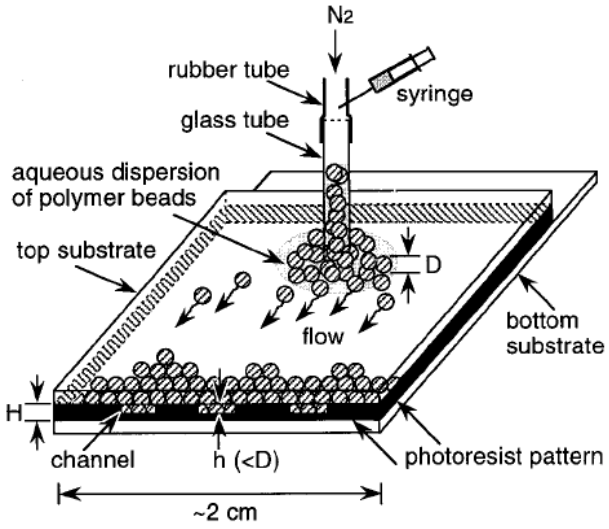

Figure 2.12: Method used by Park and Xia to obtain close packed structure with colloidal particles [31]

As can be seen from the figure, the beads are suspended in a liquid and are flowed through a channel containing a weir to capture the suspended beads. While the beads are being captured by the weir, the device is being sonicated so that the beads are forced into their thermodynamic minimum and form a ccp lattice structure. The results of this are shown in Figure 2.13.

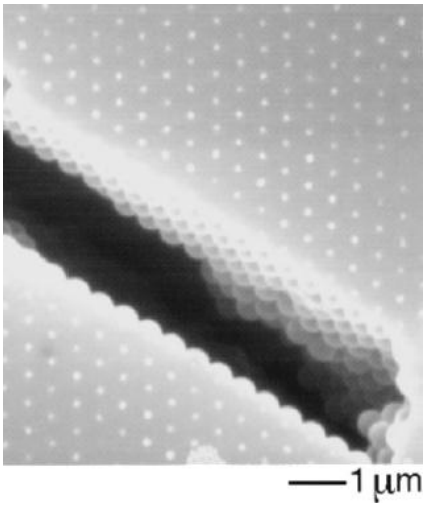

Figure 2.13: Close packed colloidal particles obtained through using Xia and Park's method

This figure shows the high level of ordered packing that is able to be achieved using this method. However, in this study the technique was performed with spheres 1 µm and smaller.

Another method for producing close packing is through vibration. Using this process, it is possible to pack much larger spheres than with other forms. The system used by Li et al for this is shown in Figure 2.14 [32].

Figure 2.14: Setup used for packing large spheres by Li et al [32]

In this study, vibrations occurred in three different axes which caused the spheres to move to their thermodynamic minimum as in the system reported by Park and Xia using sonication. Here, however, the beads that were used had a diameter of 5 mm. It was found in this study that the packing density increased as the amplitude of packing increased. It was also found that the optimal packing frequency varies depending on what vibrational amplitude is used. Although

this study specifically focuses on using large beads, the same fundamentals should be able to be applied to smaller spheres as well.

Organized packing has also been performed using methods such as sedimentation in a force field [33] and using electrostatic repulsive forces [34], but these methods of packing are generally reserved for particles in the range of 50 nm- 1 μm rather than particles that are approximately 50 μm like in this application.

Chapter 3 Materials and Methods

3.1 Methods overview

To construct the porous hydrogel scaffold to be used for non-invasive glucose sensing, many options were available as described in section 2.1.2. When comparing the different options for scaffold production, it became clear that few were able to achieve monosdispersity of pores, interconnectedness of pores, and a highly ordered packing structure. The scaffold that was created by Professor Ratner's group using PMMA microspheres as templates, however, was able to accomplish these goals [10]. Unfortunately, the use of toxic solvents to dissolve the PMMA microspheres means that this scaffold construction method cannot be used for non-invasive glucose sensing. As an alternative, a similar method using microspheres that can be dissolved using a biocompatible solvent is desirable. To do this, templating alginate microspheres can be created using microfluidics, which can then be dissolved out of the scaffold using a non-toxic solvent. The process shown in Figure 3.1 is the general method used to create the scaffold.

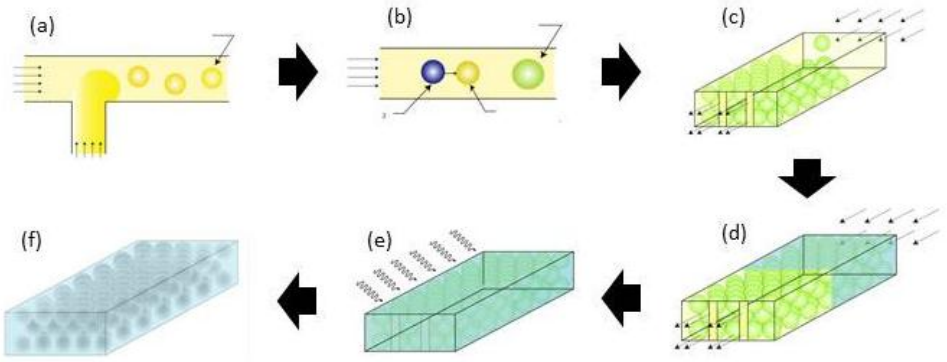

Figure 3.1: Process used to create the porous hydrogel scaffold: (a) drop production, (b) coalescence and polymerization, (c) packing spheres, (d) flow hydrogel over spheres, (e) UV polymerization, and (f) Rinse with EDTA

The first step in the process is to create monodisperse alginate drops. As described in section 2.2, there are several options for how to create drops on the order of 50 microns including flow focusing, T-junction, and co-flowing. Since the microfluidic device fabrication method carried out in our lab is mainly soft lithography, T-junction and flow focusing are our optimal options. Originally flow focusing was the preferred method due to its flexibility with the drop size obtainable through varying flow rates. Since the size of the drops is dependent on the flow rates, small variations within the syringe pumps can cause a large shift in the size of the drops. For our particular application, only single drop size is required (i.e. 30-50 um in diameter), so

the added flexibility of the flow focusing device is not necessary. Instead, a T-junction is a more desirable method for creating the drops because monodispersity is easier to obtain.

After creation of the alginate drops, polymerization of the drops is necessary through coalesce with calcium chloride as shown in equation 3.1.

3.1 $$2\,Na\ alginate\,(l) + CaCl_2(l) \rightarrow Ca\ alginate\,(s) + 2\,NaCl(l)$$

As described in section 2.3, there are many methods to facilitate drop coalescence, but each has specific limitations. The double T-junction used by Jin et al. has been successfully used for similar applications, but the consistency required is lacking because the drops do not always alternate between alginate and calcium chloride droplets, resulting in polydisperse alginate spheres [30]**.** The method used by Huang et al. is a good alternative since it is very simple and easy, but when used in practice the alginate drops often coalesce before polymerization takes place [28]. To solve this problem it is necessary for the calcium chloride to interact with the alginate immediately after the alginate droplet production. To do this, a new design was created that injected calcium chloride into the area where the alginate drops leave the channel where they were created.

There were also several options for packing the microspheres correctly. Using a vibration platform or sonication would be the most practical methods for the desired application. In order to watch the microspheres under the microscope as they pack, using sonication is preferable over a vibration stage. For each of the steps shown in Figure 3.1, there was a great deal of optimization that took place in order for the system to work correctly.

3.2 Microfluidic device fabrication

3.2.1 Microfluidic device fabrication materials

Four inch silicon wafer from Wafer Works corp, Spin coater model P6700 from Specialty Coating Systems Inc., SU-8 2035 Microchem, Torrey Pines Scientific hot plate, Heidelberg μPG 101 laser pattern generator, tridecauoro-1,1,2,2 tetrahydrooctyl trichlorosilane from Gelest Inc., peroxide-cured silicon tubing purchased from Cole Palmer with an inner diameter of 0.76 mm, Testors non-toxic cement for plastics, Polydimethylsiloxane (PDMS) from Sylgard is mixed

at a 10:1 ratio with Sylgard PDMS initiator, Diener Electronic Femto plasma chamber, precleaned 75 x 50 x 1 mm glass microscope slides from Fisher Scientific

3.2.2 Microfluidic device fabrication method

When performing microfluidics, the first step is to create a microfluidic device. The process used to do this is soft lithography, which is very useful because it allows for new microfluidic devices to be made quickly and consistently.

The first step in creating a microfluidic device is to create a template for the microfluidic device on a four inch silicon wafer. To create the mold, a spin coater is used to spread an even layer of SU-8 2035 with a thickness of 50 microns across the wafer. The wafer is then heated up to 95 degrees Celsius on a hot plate so that a soft bake of the SU-8 can take place. The SU-8 on the wafer is then exposed using a Heidelberg μPG 101 laser pattern generator. For this to happen, a CAD file is uploaded onto the Heidelburg μPG, and then the laser exposes the light sensitive SU-8 in the shape of the microfluidic device design as commanded by the CAD file. Since SU-8 is a negative photo resist, it hardens in the presence of light while the rest of the wafer that is not exposed remains soft. The wafer is next placed in a standard SU-8 developer so that the area not exposed to the laser will wash away. To finish the process of creating the microfluidic device template, the wafer is heated to 95 degrees Celsius so that the remaining SU-8 is hardened. The wafer is subsequently surface treated by placing 2 drops of tridecauoro-1,1,2,2 tetrahydrooctyl trichlorosilane into a desiccator with the wafer. This process results in a wafer that has a 50 micron thickness in the areas where the channels will be, and a bare wafer in all other locations. This can then be used as a template to create hundreds of microfluidic devices.

Using the silicon wafer just described, the microfluidic device can then be created. The initial step to do this is to glue peroxide-cured silicon tubing purchased from Cole Palmer with an inner diameter of 0.76 mm onto the inlet and exit ports of the microfluidic channels using Testors non-toxic cement for plastics. Next, polydimethylsiloxane (PDMS) from Sylgard is mixed at a 10:1 ratio with Sylgard PDMS initiator. With the tubes in place, 100 grams of the mixture is poured onto the silicon wafer to create a PDMS thickness of approximately 8 mm. The wafer with the PDMS is then placed under vacuum to remove bubbles from the PDMS mixture. The device can then be placed in an oven at 65 degrees Celsius for 1 hour which causes the PDMS to solidify. At this point, the hardened PDMS can be removed from the wafer by cutting through

the PDMS and peeling it off of the wafer. This PDMS is then placed into a Diener electronic plasma chamber with another slab of PDMS at power of 20 W and pressure of 180 mTorr for 30 seconds. After the plasma bonding is complete, the two PDMS pieces are placed together and stay bonded together. Finally, the device is placed on a hot plate at 110 degrees Celsius for 5 minutes, which completes the microfluidic device fabrication. Figure 3.2 is a picture of a microfluidic device after fabrication.

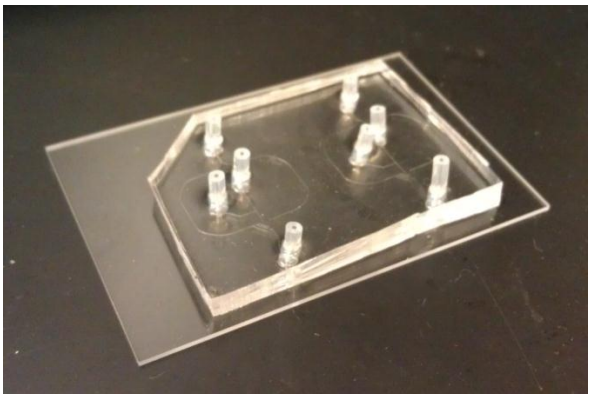

Figure 3.2: Microfluidic device after fabrication.

3.3 Experimental materials

To create the polymerized alginate drops, 2wt% low viscosity alginic acid sodium salt from brown algae purchased from Sigma Aldrich in powder form was mixed with DI water. Calcium chloride from J.T. Baker was also mixed at a concentration of 5wt% with DI water, and liquid Span 85 from Fluka was mixed with soybean oil produced by Cibaria at a concentration of 0.5% by volume. All three of these fluids were then placed in 3 mL BD plastic syringes which had BD precision guide sub-Q 26G needles attached to the end. Polyethylene tubing with an inner diameter of 0.38 mm from Intramedic was then placed on the end of the needles which was inserted into the microfluidic device. To ensure that the channel is hydrophobic, Rain-x produced by SOPUS Products is flowed through the channel. One Harvard Apparatus PHD 2000 Infusion syringe pump and two Milliliter OEM syringe pump modules from Harvard Apparatus were then used to control the flow rate of the Rain-x as well as the other fluids. To watch the fluids while they travel through the microfluidic device, a Leica DMI 3000B microscope is used with an attached Photron Fastcam-X 1280PCL model 16KC high speed camera.

After the polymerized alginate spheres are created, they are packed into another microfluidic device. This device is placed in a BD Falcon 100 mm diameter x 15 mm deep petri

dish with DI water covering the device. The packing then takes place through placing a Sonics Vibracell VCX500 sonication horn within 1 cm of the device to move the spheres to their thermodynamic minimum. The sonication generator has a power of 500W and runs at a frequency of 20 kHz and the model of the horn itself is CV33. During the sonication the alginate spheres are flowed into the channel using the same syringe pump system as described before, or through creating suction from the outlet with a 10 mL plastic BD syringe while the drops enter the device through a funnel.

The alginate microspheres are then rinsed using isopropyl alcohol from Macron Chemicals by using the syringe pump system. Following the rinse, the hydrogel is flowed over the drops using the same procedure. The hydrogel solution was prepared by mixing 43vol% DI water**,** 51vol% 2-Hydroxyethyl methacrylate from Polysciences Inc., 4.6vol% Etheylene glycol from Sigma Aldrich, 1.9vol% Tetraethylene Glycol Dimethacrylate from Polysciences Inc., and 0.8wt% 2,2 Dimethoxy-2-phenyl-acetophenone from Sigma Aldrich. Following the hydrogel flowing over the spheres, the microfluidic device was placed under a UV light from UVP was which had a power of 15 Watts and a wavelength of 254 nm for one hour to polymerize the hydrogel. After removing the polymerized hydrogel from the microfluidic device, the scaffold is soaked in 0.125M Ethylenediaminetetraacetic acid (EDTA) from Sigma Aldrich for 4 days to dissolve out the alginate. While the scaffold soaks in a vial of EDTA, the vial is periodically sonicated with a Branson 2510 sonication bath to remove the dissolved alginate.

Chapter 4 Results

4.1 Monodisperse solid alginate drop production as templating spheres

To make consistent 50 μm drops of alginate in oil, there are many steps and it is extremely important to use the proper two immiscible fluids that provide good interfacial tension and viscosity ratio to facilitate droplet formation as described in section 2.2.

4.1.1 Flow Parameters

After the microfluidic device has been created, there are several parameters to control before it is possible to make monodisperse alginate droplets with a diameter of 50 μm.

The first parameter to control is the flow geometry itself in order to produce drops that are the correct size. One of the advantages of the T-junction is that there are very few geometric variables that need to be optimized. As long as w_c (continuous phase channel width), w_d (dispersed phase channel width), and w_o (channel width after droplet production) in Figure 2.7b are all the same size as the desired drop diameter, it will be possible to create drops similar to the channel width. The fluid properties as well as the flow rates still remain important parameters even if the geometry is correct.

4.1.1.1 Fluid Properties

The first fluid property that needs to be taken into consideration is the viscosity of the alginate solution. The alginate used here and in all other studies is a low viscosity alginic acid sodium salt from brown algae purchased from Sigma Aldrich in powder form. The alginic acid powder was then mixed with DI water in different concentrations to form an aqueous solution. Within microfluidics, it is much easier to reach desired results if a Newtonian fluid is used. If not, the viscosity will change while the flow rates change, making fine tuning of the system very difficult. In order to check to see whether the alginate is Newtonian, a TA instrument stress controlled AR 2000 rheometer was used to test the shear viscosity at a range of shear rates that would be expected to occur within the microfluidic device. To find the shear rate, the average velocity in the channel first needs to be found using equation 4.1.

4.1
$$v_{avg} = \frac{Q}{A} = \frac{50\ \left[\frac{\mu L}{hr}\right]}{50\ [\mu m] \times\ 50\ [\mu m]} = 0.018\ \frac{m}{s}$$

Using the average velocity, the approximation for the shear rate is shown in equation 4.2.

4.2 $$\dot{\gamma} \approx \frac{v_{avg}}{l} = \frac{0.018\left[\frac{m}{s}\right]}{50\ [\mu m]} = 367\ s^{-1}$$

Here $\dot{\gamma}$ is the shear rate and l is the characteristic length, which, in this case, is the channel width. This calculation shows that a shear rate of 367 1/s is present during our experiments. This is consistent with other studies which report shear rates between 40 and 600 1/s [35-37]. Knowing this information, it was then possible to test the appropriate shear rates using the rheometer. Figure 4.1 shows the plot of shear viscosity versus shear rate for three different concentrations of alginate in DI water.

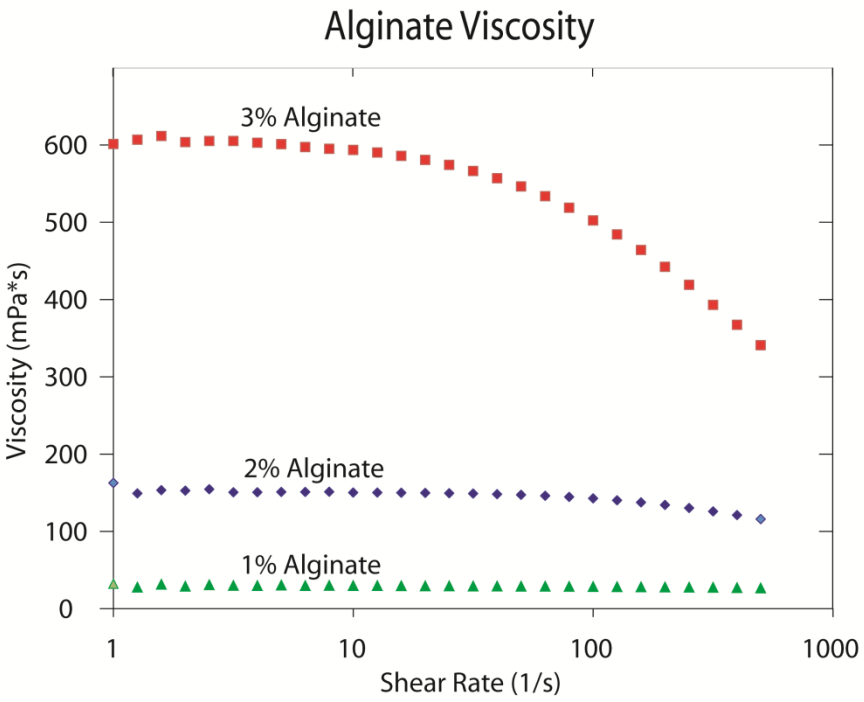

Figure 4.1: Shear viscosity for varying alginate concentrations and shear rates.

In the figure, the 3% alginate shows shear thinning behavior, while the 1% and 2% alginate exhibit relatively Newtonian behavior over the range of shear rates expected within the microfluidic device. In a study performed by Huang et al., alginate drops were made in a T-junction with a viscosity of 255 mPa*s [27]. In order to mimic their study as closely as possible,

2% alginate was used for our experiments because the zero shear viscosity of that concentration was closer to 255 mPa*s than the 1% alginate zero shear viscosity.

The continuous phase viscosity is another important parameter when creating drops. In the study mentioned previously by Huang et. al, the viscosity ratio between the dispersed and continuous phase was $\lambda \approx 5$ [27]. When using 2% alginate as the dispersed phase, the continuous phase should have a viscosity on the order of about 30 mPa*s. It is also extremely important that the continuous phase and dispersed phase are immiscible. Using these criteria, vegetable oil was used which is a Newtonian fluid with a zero shear viscosity of 55 mPa*s.

The next primary fluid property to consider is the interfacial tension between the continuous phase and the dispersed phase. As discussed in section 2.2, it is necessary for the capillary number to be in the range of $2.2 \times 10^{-2} \leq Ca \leq 1.1 \times 10^{-1}$ for droplet breakoff to occur in a T-junction [19]. Since the capillary number is a balance between viscous stresses and interfacial stresses, and the viscosity is already known, it is then possible to see whether drops can be formed within the microfluidic device with the interfacial tension between the two fluids. Using a KSV Sigma tensiometer, the interfacial tension was measured to be 9 mN/m between the vegetable oil and 2wt% aqueous based alginate solution. Using this interfacial tension along with the flow rates found to be successful in Huang et al. [28] and the viscosity of the alginate, the capillary number was found to be 9.16×10^{-2} as shown in equation 4.3.

4.3
$$Ca = \frac{\mu U}{\sigma} = \frac{(150 \times 10^{-3}\,[Pa * s])\left(0.055\left[\frac{m}{s}\right]\right)}{9 \times 10^{-3}\left[\frac{N}{m}\right]} = 9.16 \times 10^{-2}$$

The capillary number here fits the range that was cited in Tice et al [19], which means that droplet production should be possible with our fluid selections. The interfacial tension was eventually lowered by adding a surfactant due to coalescence reasons that will be discussed in section 4.3. To do this, 0.5% Span 85 from Sigma was added into the oil which lowered the interfacial tension to 6 mN/m. The result was a capillary number of 1.38×10^{-1} which still falls in the acceptable range of capillary numbers.

4.1.1.2 Flow Properties

After the geometry and the fluid properties have been optimized, the flow rates still need to be adjusted in order to create monodisperse alginate drops. Using the study performed by Huang

et al. [27] as a reference point, the continuous phase was initially set at 120 μL/hr while the dispersed flow rate was set at 50 μL/hr. Figure 2.8 created by Grastenecki et al., shows that the dispersed phase flow rate should be approximately 40% of the continuous phase flow rate and verifies that these flow rates will produce a droplet that is the same length and width as desired [26]. Since both of these systems are slightly different from the device geometry that was being used for this application, the numbers will not be exactly the same, but it is certainly a good reference point.

To test these flow rates, the fluids were placed in 3 mL BD plastic syringes and attached to 26 gauge Sub-Q luer lock needles. Polyethylene tubing with an inside diameter of 0.38 mm was then used to connect the syringe needles to the microfluidic device. To control the flow rates through the syringes, Harvard Apparatus PHD 2000 Infusion pumps were used. Using this setup, the flow rates described previously were tested, and it was discovered that the drops that were being created were larger than 50 μm as desired. To decrease the size of drops, it was necessary to decrease the ratio of the dispersed phase to the continuous phase, which was done through increasing the flow rate of the continuous phase. After numerous experiments, it was found that the optimum flow rates in order to create 50 μm diameter drops, was a continuous flow rate of 200 μL/hr and a dispersed flow rate of 50 μL/hr. It was also found during the experiments that by keeping the flow rate ratio the same, but increasing or decreasing both flow rates, the frequency of drop production also increased or decreased. As described in the following section, being able to increase or decrease the frequency of droplet production can be extremely helpful. Figure 4.2 shows an image of the alginate drops being produced in the T-junction with the final geometry, fluid properties, and flow rates. The image shown here was taken under a Leica DMI 3000B microscope with a Photron factcam high speed camera. All of the experiments perfromed used this same microscope and camera.

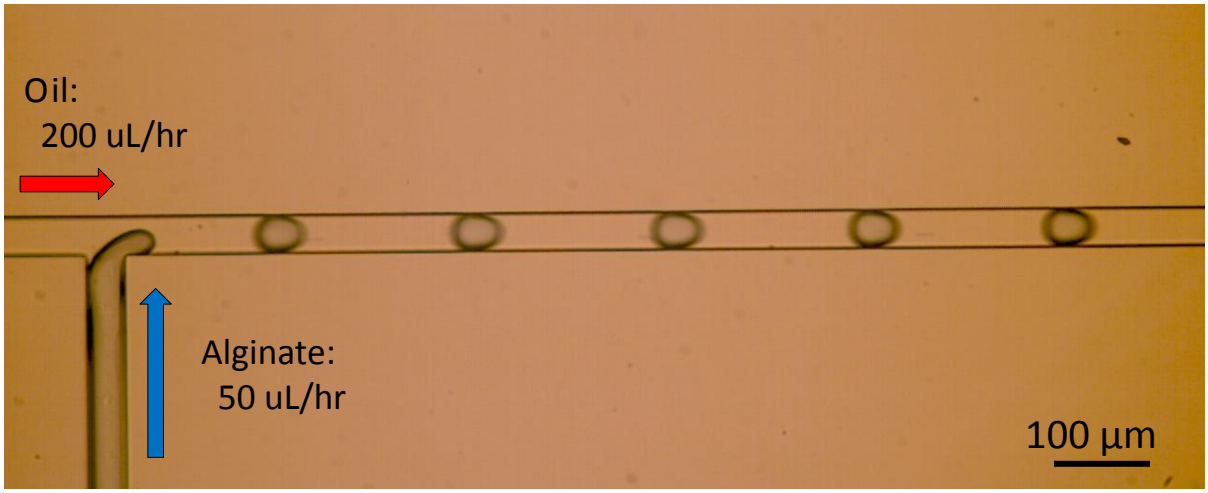

Figure 4.2: Alginate drop production

4.2 Coalescence

After attempting to use several of the methods for coalescence previously described in section 2.3, it eventually became clear that it would be necessary to use a different type of design for the alginate to coalesce with the calcium chloride. The design used and the optimization steps that were taken are described in the following sections.

4.2.1 Coalescence Method Used

The new method to enhance coalescence of the alginate drops with calcium chlorides still uses a regular T-junction to create the alginate drops as described in section 3.2. With this method, directly after the alginate drops leaving the 50 µm wide channel, a large amount of calcium chloride flows in to immediately polymerize the alginate drops. The design used to do this is shown in Figure 4.3. The red box in the figure shows where the alginate and calcium chloride enter into the same channel

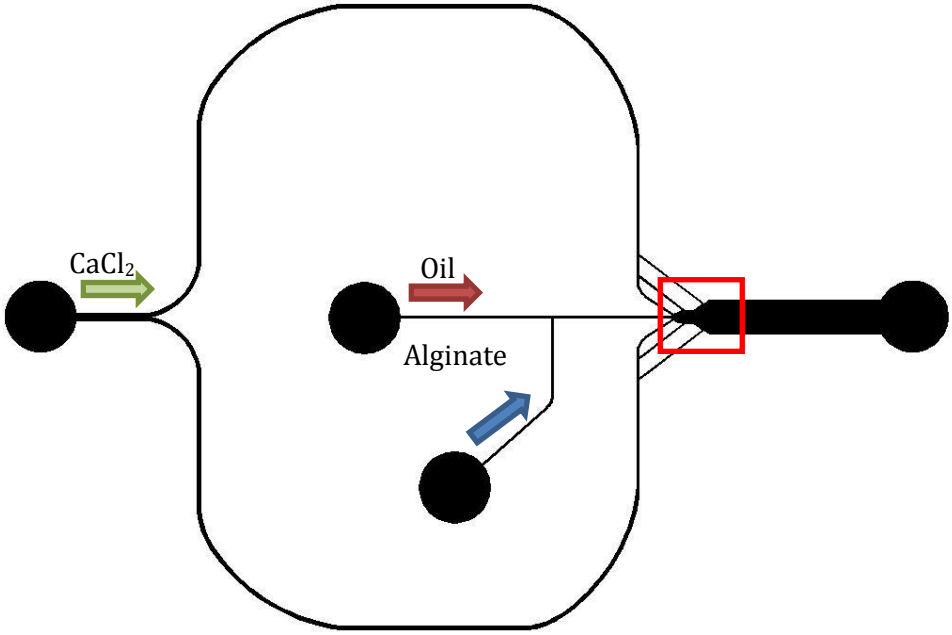

Figure 4.3: Design used to create and polymerize alginate drops.

As shown in the figure, the alginate drops are created in a normal T-junction with the alginate entering from the bottom channel, and oil entering directly above it. After the drops are created, they then flow into an expansion chamber as highlighted by the red box in Figure 4.3. The calcium chloride enters from the far left port and branches off to travel around the T-junction. Each branch then branches off again into three separate channels which all feed directly into the expansion chamber. The expansion chamber initially has a small width so that the calcium chloride will enter the channel and separate the alginate drops to make sure that they do not coalesce with other alginate drops. The channel then expands so that the drops will stay in the channel longer and assure coalescence with the calcium chloride before exiting the device. Figure 4.4 shows the expansion area when alginate drops and calcium chloride are flowing.

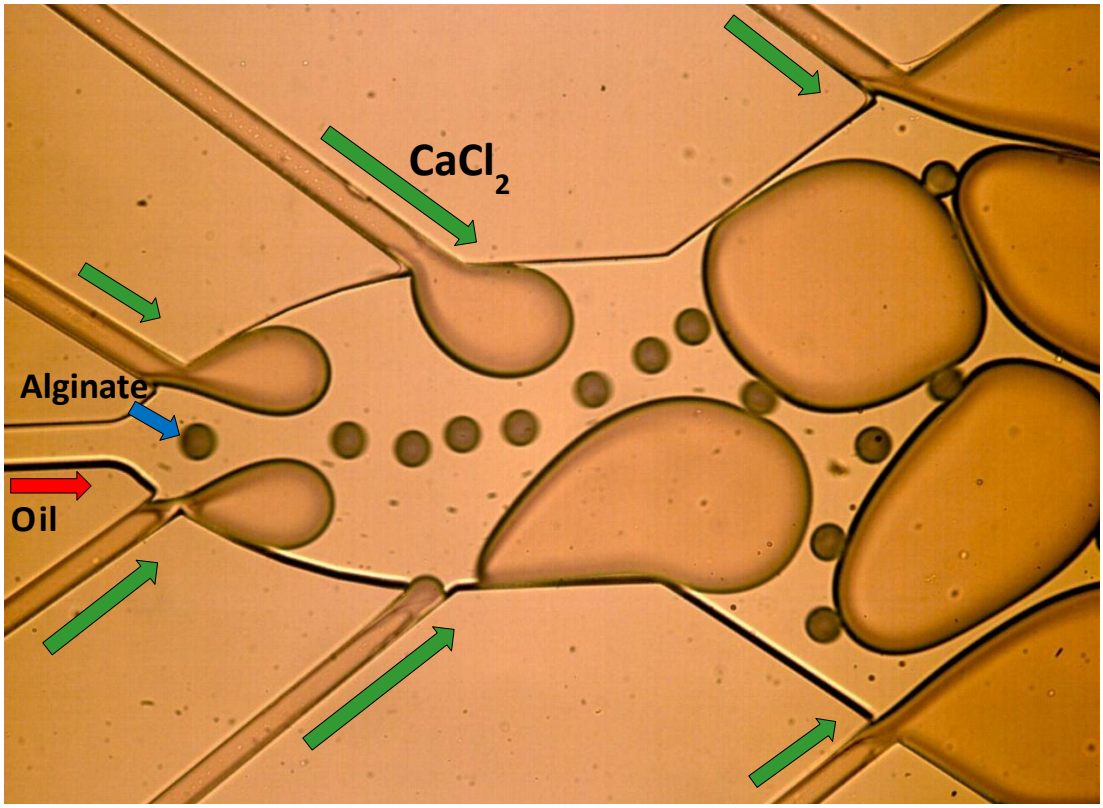

Figure 4.4: Alginate, calcium chloride, and oil entering the expansion chamber

From this figure it can be seen that the alginate drops do not immediately coalesce with the calcium chloride globules, but the alginate drops also do not coalesce with other alginate drops. Further down the channel the alginate does coalesce with the calcium chloride and the alginate drops polymerize to form solid spheres. For this method to work properly, a great deal of optimization was necessary.

4.2.2 Device Optimization

The original device had 6 inlets into the coalescence chamber in order to continue to force the drops to coalesce as they traveled through the channel. This design that was used is shown in Figure 4.5.

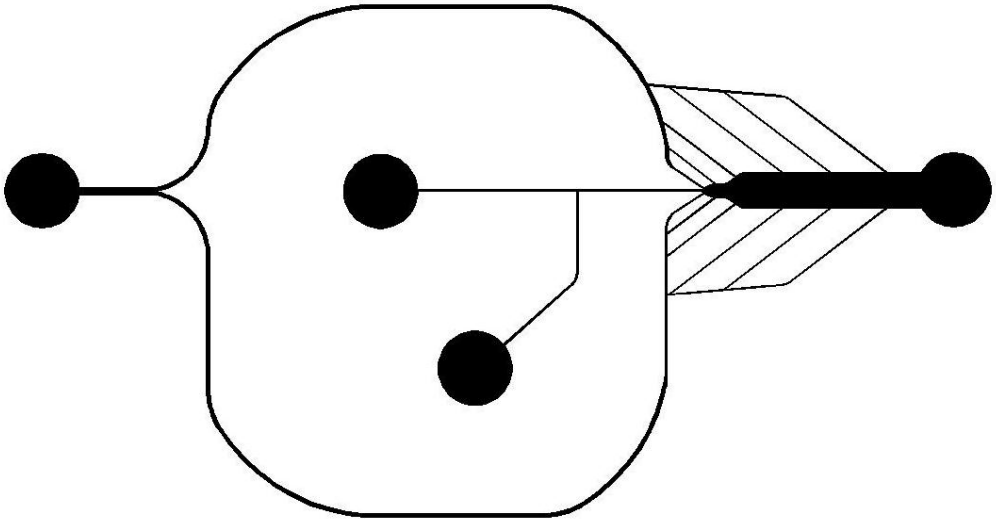

Figure 4.5: Original microfluidic design for alginate and calcium chloride coalescence

Using this device it became clear that it was not necessary to have that many inlets. It actually caused issues to arise because there was not enough calcium chloride where the alginate exited the channel since it was split between so many branches throughout the length of the device. Another problem was that there was more calcium chloride exiting the top inlets than the bottom. Before creating a new device to attempt to fix these problems, a Comsol simulation was performed to check the flow rates exiting each branch.

In order to perform the simulation, there were many simplifications made so that the model would run more efficiently. The first assumption was that the system consisted of only one single phase fluid instead of alginate, oil, and calcium chloride. Dealing with multiphase flow is challenging and computationally intensive, and since only the volumetric flow rates of the calcium chloride were being studied, this is a legitimate approximation to make. The T-junction was also removed and replaced with a single inlet because the T-junction itself does not alter flow of the calcium chloride. All of the inlets were also assumed to be a flat face rather than a circular inlet like in the actual device. Since the length of the channels before the entrance of calcium chloride is longer than the length of the developing region, this is also a legitimate approximation. Using these approximations, the geometry shown in Figure 4.6 was used.

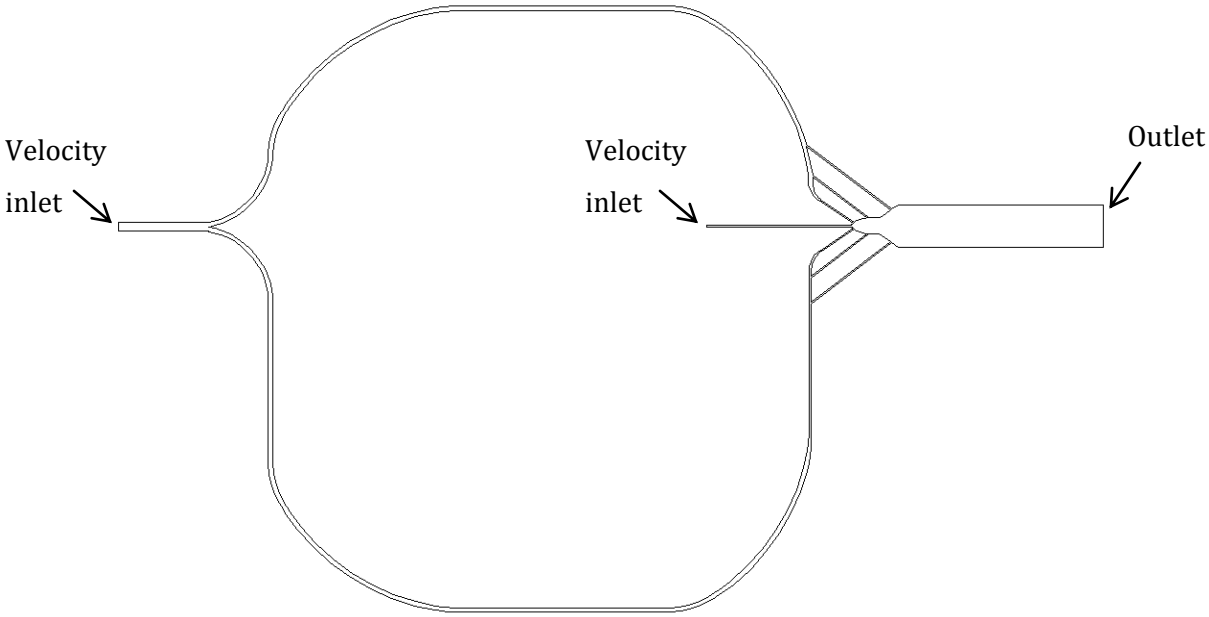

Figure 4.6: Simplified geometry used for CFD analysis

Within the model, there were two velocity inlets and one outlet as shown in Figure 4.6. The rest of the boundary conditions were set as no-slip walls. It was also necessary to create an appropriate mesh for the system. The area that had the most refined mesh was the expansion chamber where the calcium chloride entered the system. Figure 4.7 shows the mesh that was used in that expansion area.

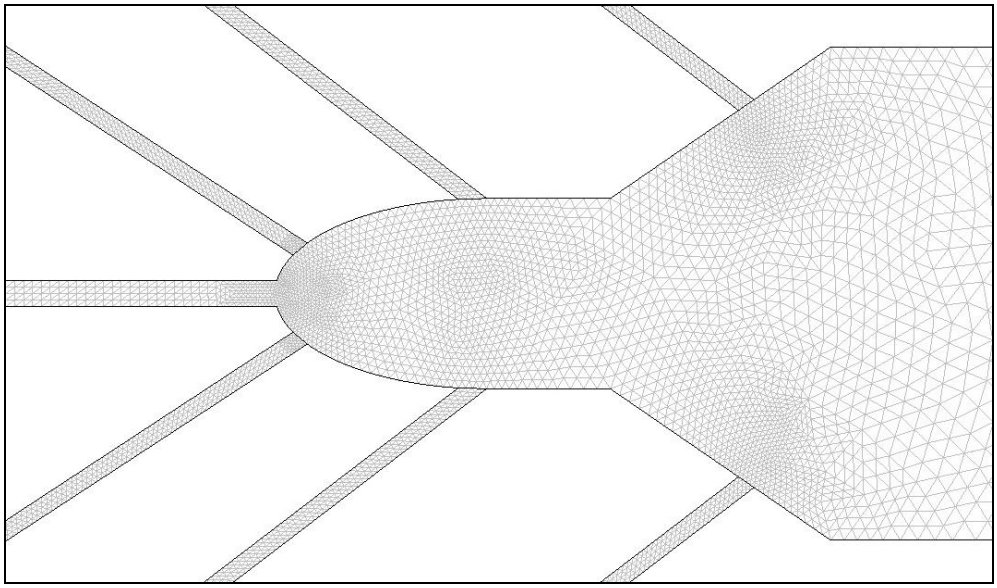

Figure 4.7: Mesh used in the expansion area where the calcium chloride enters

The mesh here is much finer in the channels and in the areas where the channels enter the expansion area than in the rest of the device. By having a finer mesh in the areas where more activity takes place in the flow, the computational model is more accurate. Using this mesh and the boundary conditions described, the following velocity field shown in Figure 4.8 is obtained.

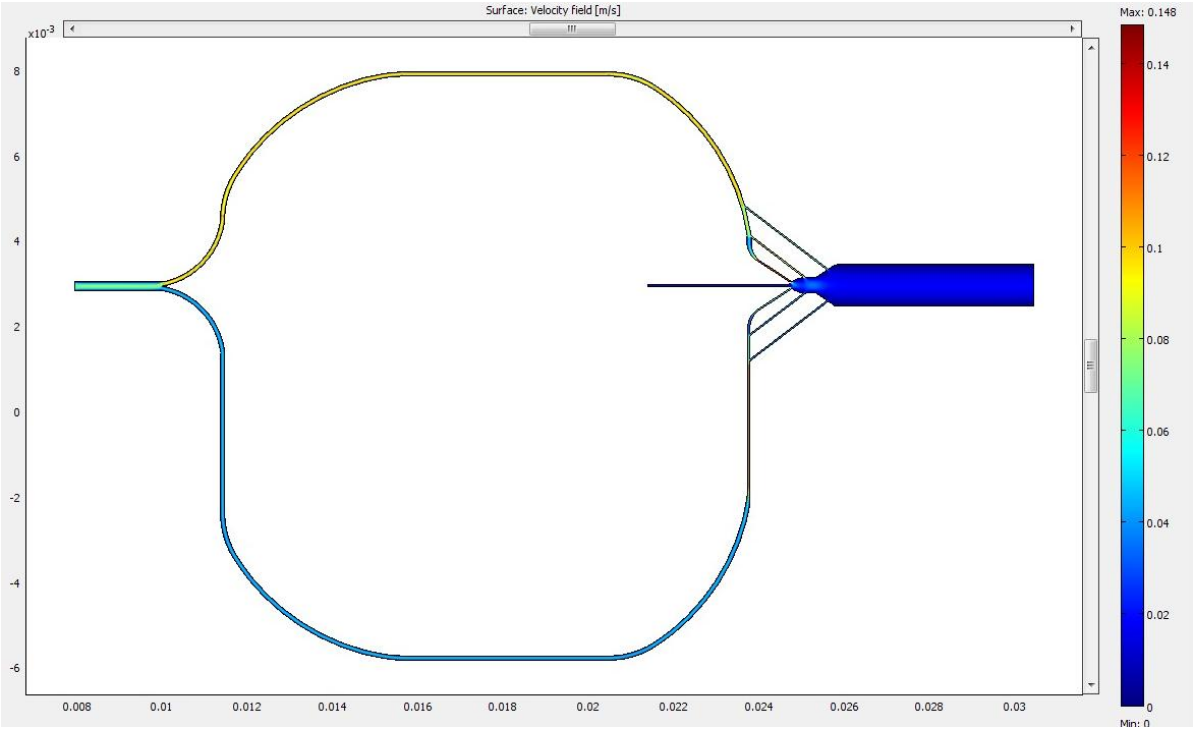

Figure 4.8: Velocity field for the original channel design

In this figure, it is difficult to see the where the branches feed into the expansion area which is the area of interest. Through analyzing this figure, it is possible to see that the velocity is higher in the top channel than in the bottom. Through looking at the close up of the expansion area in Figure 4.9, the fluid velocity is greater through the top than the bottom as well.

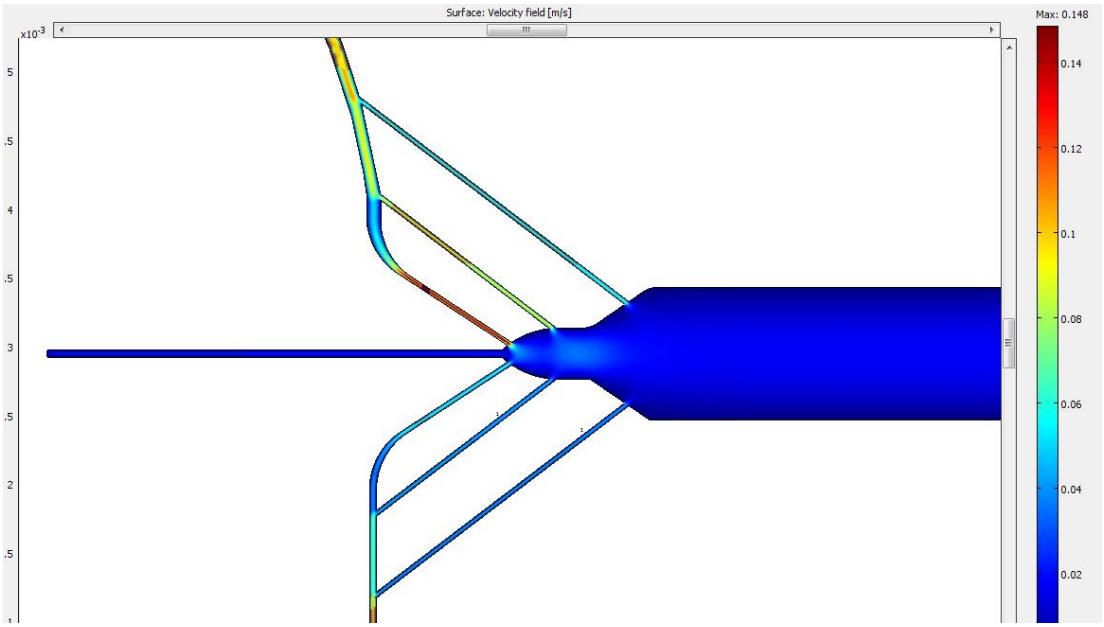

Figure 4.9: Velocity field for the expansion area of the original design

In order to equalize the flow rates in the top and bottom channels, a new design was analyzed that had the exact same channel on the top as the bottom. With the current design, the top channel was shorter than the bottom channel resulting in a difference in the pressure drop between the two channels, which lead to a difference in the mass flow rates. The symmetric design that was used is shown in Figure 4.6. The velocity field for the expansion area of this device is shown in Figure 4.10.

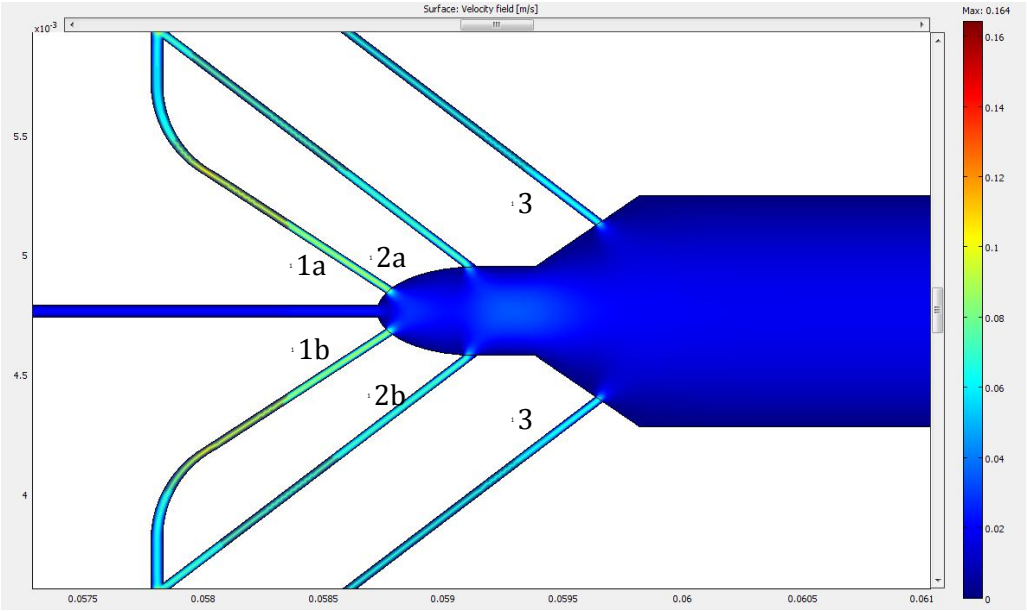

Figure 4.10: Velocity field for the expansion area in the symmetric channel design

This figure shows that the symmetric channel does cause a symmetric flow through the channels. Since it is important to have approximately equal flow rates through each of the channels, it is also necessary to find the volumetric flow rate entering the channel at each of the branches. To complete this analysis, a boundary integration of the velocity was performed where the calcium chloride enters the expansion chamber. The result of the integration is a volumetric flow rate. This was then converted into a percentage of the total flow rate so that it would be easier to characterize the flow rate distribution. This was performed for both the original design as well as the symmetric design and compiled into Table 4.1.

Table 4.1: Flow percentage through calcium chloride channels in two different designs found using Comsol

Channel Number	Original design	Symmetric design
1a	32.6	19.8
2a	22.5	18.8
3a	11.4	14.8
1b	12.9	19.4
2b	10.7	18.7
3b	7.7	14.7

This table shows how greatly the symmetry of the calcium chloride channels affects the distribution of the calcium chloride. The percentage of flow that is occurring through the bottom of the channel is nearly identical to the flow that is occurring through the top in the symmetric design, while original design contains an extremely large discrepancy. The flow rates are consistent through each of the channels going from left to right in the symmetric channel as well. The computational results show that the flow distribution is evenly distributed enough in the symmetric design that more optimization is not necessary.

4.2.3 Flow optimization

After optimizing the flow geometry, the new symmetric channel design shown in Figure 4.6 was fabricated. To polymerize the alginate drops in this device, the first step was creating droplets in the T-junction using the same method as described in section 4.1. As monodisperse alginate drops were created, calcium chloride was flowed into the device to cause coalescence with the alginate droplets, resulting in polymerized spheres. To find the optimum calcium chloride flow rate to use, experimentation was necessary since there was no data available from any similar devices. Through experimenting with different flow rates, it was found that using a calcium

chloride flow rate too low (approximately 500 μL/hr) resulted in too little calcium chloride flowing into the expansion area to separate the streams of calcium chloride. This meant that there were streams of approximately 7-8 alginate drops directly next to each other, leading to a higher probability of alginate drop coalescence before coalescing with the calcium chloride. Using a flow rate that was too high (approximately 1500 μL/hr), caused problems as well. Instead of the calcium chloride entering the channel and separating the stream of alginate drops, the calcium chloride stayed along the side of the channel and did not interact with the alginate. When this occurred the alginate drops were not separated at all which caused more polydispersity issues than using the lower flow rate. By using a flow rate of 1200 μL/hr, both of these problems were eliminated as there was enough calcium chloride supplied to separate the alginate drops, but not a flow rate too high to change the flow characteristics. The result of using this flow rate was shown previously in Figure 4.4.

4.2.4 Fluid optimization

Although using these flow rates gave the desired flow pattern, more refinement of the system was necessary in order to obtain the proper coalescence of calcium chloride and alginate droplets. When dealing with coalescence of two fluids, the interfacial behavior between those two fluids and the continuous phase is extremely important. In the original system that contained 2% alginate, 5% calcium chloride, and vegetable oil as the continuous phase, the interfacial tension between the two immiscible fluids and the oil was 9 mN/m which was too high, giving much higher resistance to coalescence. The result was that the alginate drops initially resisted coalescence and deformed before coalescence took place. Since the polymerization time between alginate and calcium chloride is very short, the polymerized alginate took the form of the deformed drops rather than a spherical drop as desired. To eliminate this problem, a surfactant (0.5% Span 85 by volume), was added to the oil phase to lower the interfacial tension to 6 mN/m. By doing this, the coalescence between the alginate and calcium chloride occurred much more easily and resulted in much more consistent spherical droplets. If too much Span 85 was used in the oil, the alginate drops began to coalesce before having the opportunity to coalesce with the calcium chloride. This again led to a high polydispersity of the alginate drops. Using a concentration of 0.5% Span 85 was found to be the most successful concentration of surfactant to use in order to produce monodisperse alginate microspheres. Figure 4.11 shows an image of the polymerized alginate microspheres produced after leaving the device. In this figure the polymerized alginate spheres are the small circular

objects contained within the large liquid calcium chloride drop. The blue arrow indicates one of the many polymerized alginate spheres

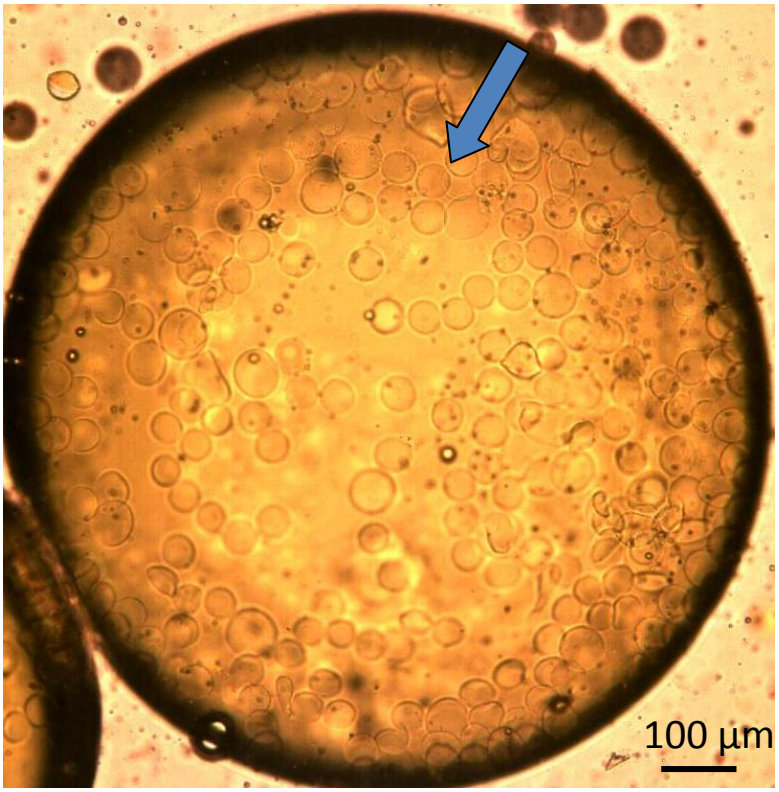

Figure 4.11: Polymerized alginate spheres suspended within a calcium chloride drop on a glass slide. One of the many alginate spheres is indicated by the blue arrow.

The alginate spheres in this figure are very spherical and monodisperse. The size of these spheres is 35 µm, which is exactly between 30 and 40 µm as desired. These alginate spheres were imaged with the scanning electron microscope (SEM) to ensure that they were really spheres and not just disks. To perform the SEM imaging, the oil needed to be removed from the oil. To do this, the solution of calcium chloride, oil, and alginate spheres was centrifuged at 3500 rpm for 5 minutes. The top half of the liquid was then removed, replaced with isopropyl alcohol, and then centrifuged again. This same process was done three times, and then the alginate drops were removed with an eye dropper from the bottom of the centrifuge container. These drops were placed on a glass slide and then dehydrated in an oven at 65 degrees C for 3 hours. Next, the slide of drops had a lead and gold sputter coating placed on it to make the drops conductive. After this occurred, an FEI Sirion SEM was used to image the spheres at a working distance of 7.6 mm and a magnification of 2972x. Figure 4.12 shows an SEM image of the polymerized alginate sphere.

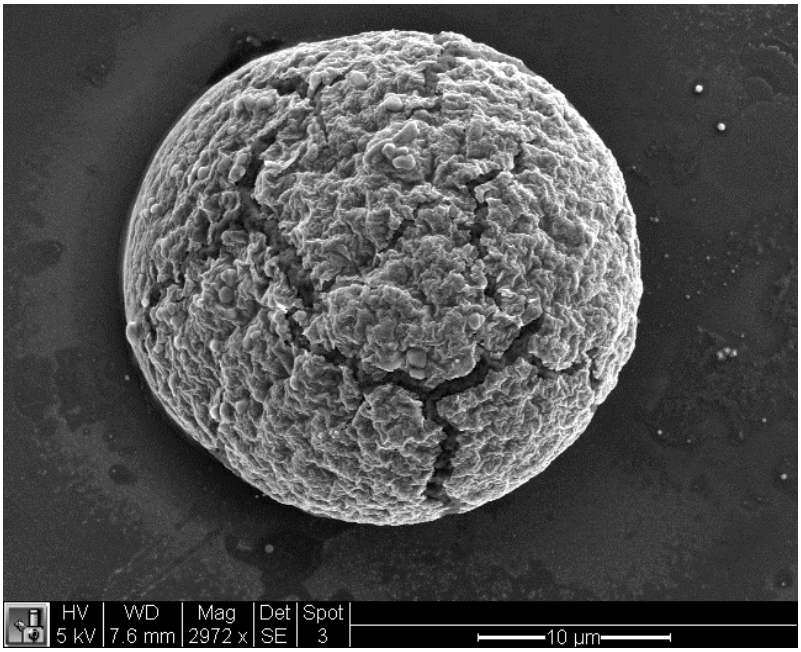

Figure 4.12: SEM image of an alginate microsphere

This image shows that the alginate spheres are actually spherical. Cracking can be noticed on the sphere which is most likely due to the necessary drying of the alginate prior to imaging.

4.2.5 Microsphere rigidity optimization

Using the geometry, fluids, and flow rates described above, monodisperse alginate drops were produced, but it was also extremely important that the microspheres have a high degree of rigidity for packing. If not, the drops will deform when packed and lose the spherical shape that is required within the scaffold. The alginate spheres produced using 5% calcium chloride and 2% alginate did not offer enough rigidity to pack correctly. Using higher concentrations of calcium chloride creates more rigid structures, but the alginate microspheres formed are not as spherical when using a higher concentration. To ensure fully spherical alginate microspheres, 5% calcium chloride was used to polymerize the alginate. Those microspheres were then flowed directly into a vial containing 30% calcium chloride where they were able to soak before being packed. While soaking in the vial, the spheres were continually stirred to ensure that flocculation of the particles would not occur. Through using this method, the rigidity of the spheres was increased greatly. A set of experiments was performed to find the correct length of time and concentration of calcium chloride to soak the drops to create the most rigid alginate microspheres.

To test the rigidity of the alginate spheres, a bulk test was performed. Using a micropipette, alginate drops were created and dropped into a vial of 20 ml of 5% calcium chloride to mimic the process alginate microsphere production in the microfluidic device. The drops were then removed and soaked in 10%, 20%, 30%, and 40% calcium chloride by weight for .5, 1, 2, 3, 5, 24, and 72 hours. After soaking in calcium chloride, the alginate spheres were removed, placed on a glass slide, and an image was captured of each sphere individually with a Canon PowerShot SD890 IS Digital Elph camera. A glass slide was then placed on top of each alginate sphere to test the compressibility of the sphere. When the slide was placed on the sphere, an image was immediately taken, and subsequent images were taken every 30 seconds to capture the alginate sphere compression with time. After 5 minutes, the weighted slide was then removed and images were taken every 30 seconds for 2 minutes in order to see whether the drops regained their original shape after deformation. The height of the drop was then measured from each image using ImageJ. Using the height of the spheres found in the images, it was then possible to find the total deformation that occurred over time with spheres made using different concentrations of concentrations and different soak times. For each of the tests that were performed, three alginate spheres were tested under the same conditions in order to see the variation of the data collected. An example of one of the droplet deformation tests is shown here in Figure 4.13. For this test, the alginate sphere was created in 5% calcium chloride, left in the solution for 30 seconds, then placed in 10% calcium chloride for 30 minutes, and finally removed and tested.

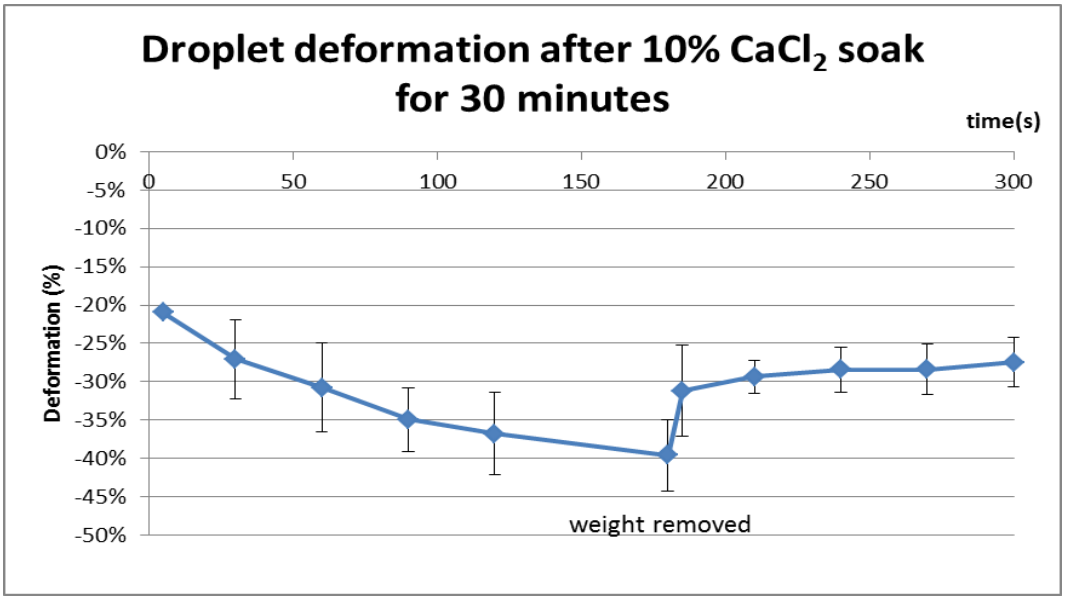

Figure 4.13: Droplet deformation for alginate spheres soaked in 10% calcium chloride as a function of time.

In this figure, the droplet deformation is shown as a function of the time after the weighted slide was initially placed on the alginate sphere. Here the alginate sphere continues to compress the longer that the slide is on the sphere. At three minutes the weight was removed, and then some of the deformation was recovered. The standard deviation in this figure, as shown by error bars, is small enough that the basic trends can be seen from the test. Using deformation data similar to Figure 4.13, but with different concentrations of calcium chloride and different soak times, the maximum deformation was plotted as a function of soak time as shown by Figure 4.14.

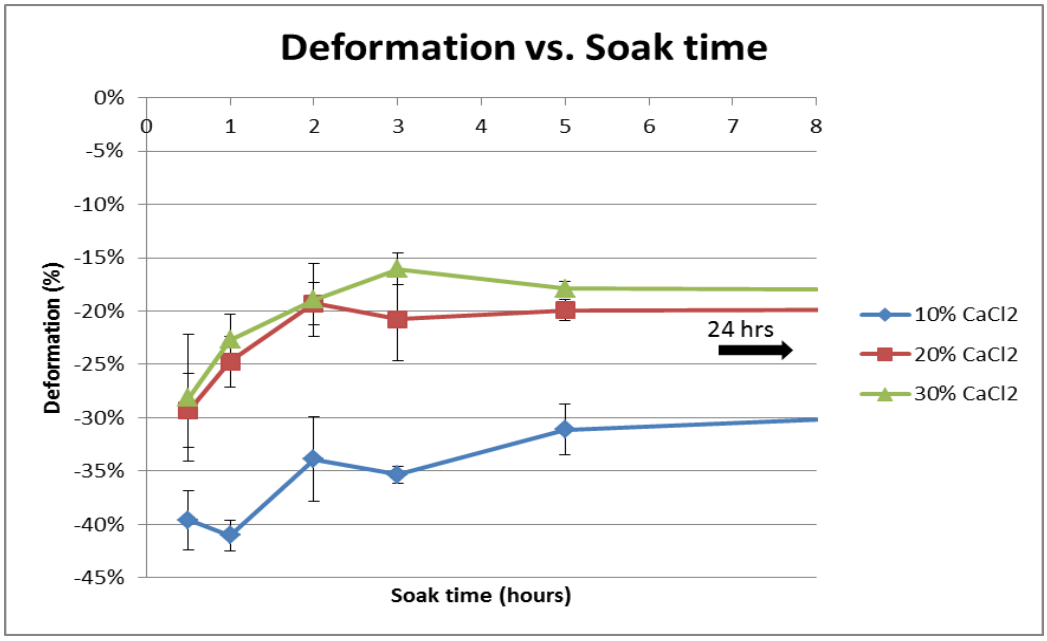

Figure 4.14: Maximum alginate drop deformation as a function of soak time

This plot shows that the longer the drops soak in calcium chloride, the more rigid they become. It also shows that using a higher calcium chloride concentration increases the hardness of the spheres. For concentrations of calcium chloride higher than 30%, however, the alginate drops deform and it is no longer possible to form spheres as desired. For this reason, 30% is the highest calcium chloride concentration that can be reasonably used to increase the hardness of the alginate spheres.

The results previously shown are all for spheres with a diameter of approximately 3 mm as opposed to 50 μm which will be used in the actual application. Although the behavior is not identical for smaller drops, the similar general trends are present. Using the collected data, the most effective method for creating rigid spheres was developed. This method was to create alginate microspheres in the microfluidic device using 5% calcium chloride and then soak the

microspheres in 30% calcium chloride for 3 hours. Through using this method, the spheres held the necessary shape and were not deformed.

4.3 Microsphere Packing

After the drops have been created, the next step is to pack all of the drops into a microfluidic channel as shown in Figure 4.15.

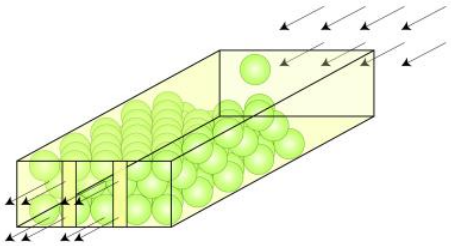

Figure 4.15: Alginate drop packing

To do this, there were a number of optimization methods required.

4.3.1 Microfluidic device selection

To pack spheres within a microfluidic channel, it is necessary to filter the spheres while allowing the fluid to continue to flow through the device. For the original tests that were performed, the drops were packed into a micropost array device. This device is represented in Figure 4.16.

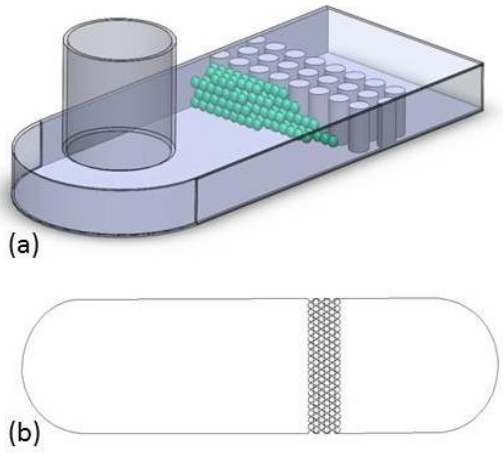

Figure 4.16: (a) Isometric view of the alginate sphere packing in a micropost array. (b) 2 dimensional drawing of the micropost array

In this device the diameter of the microposts is 100 μm with 10 μm gaps between each of the posts, while the height of the channel is 100 μm. Since 50 μm spheres were being packed in the channel, the spheres were easily filtered while the fluid was still able to flow through the device without difficulty. However, since the height of the device is only 100 μm, a maximum of two layers of spheres could pack into the channel. Also, the face that the spheres packed against was not flat, resulting in the first row of spheres not packing in an orderly manner. This then affected the packing of the subsequent layers as well. Due to both the lack of depth in the microfluidic channel and the non-flat face, a new design was necessary. In this device the depth was increased to 300 μm so that there could be six layers of packing. The face where the packing occurred was also made flat so that ordered packing could start on the first layer. This design is shown in Figure 4.17.

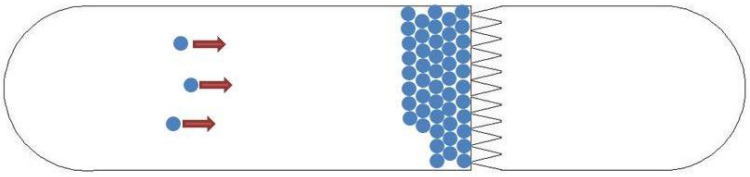

Figure 4.17: 2-dimensional drawing of the flat face packing device. Spheres flow from left to right.

4.3.2 Transferring Alginate spheres

One of the large challenges of packing the alginate spheres is finding the appropriate way to flow the spheres through the microfluidic device. After numerous trials it was found that the most effective way to transfer the alginate spheres into the microfluidic device for packing was to attach a 3 mL BD plastic syringe without the plunger to the inlet of the microfluidic device and use it as a funnel into the device. The alginate spheres are then poured into the funnel so that the alginate spheres will flow into the microfluidic device. Due to the high pressure drop that occurs in the microfluidic device, gravity alone is not enough to cause the suspended spheres to flow through the channel. To cause the spheres to flow, another syringe was placed at the exit to apply suction to the system so that the suspended alginate spheres would flow through the channel and pack.

4.3.3 Packing alginate spheres

As the drops flow into the microfluidic device, the sonication occurs so that the spheres will move to their thermodynamic minimum as the flow is occurring. As described previously,

sonication is the best method for doing this so that the drops can still be viewed while they are packing, and so that sufficient agitation is present to force the spheres into their thermodynamic minimum. The form of sonication that was used to do this was a Sonics Vibracell VCX500 sonication horn. For the sonication to work correctly the microfluidic device was placed in a BD Falcon petri dish with enough water so that the entire microfluidic device was covered. The sonication horn tip was then placed in the water so that the horn was pointing toward the area of the device where the packing was taking place. It is important that the tip of the sonication horn does not touch the bottom of the glass or the microfluidic device while the sonication horn is running. To make sure that this does not happen, the sonication horn is held in place by a series of clamps attached to a ring stand. Once the sonication horn was secured, the drops were then flowed through the channel as the sonication began at a frequency of 20 kHz and an amplitude setting of 22%. To test this method, glass spheres were first used to see whether the packing would be sufficient. The result of this is shown in Figure 4.18.

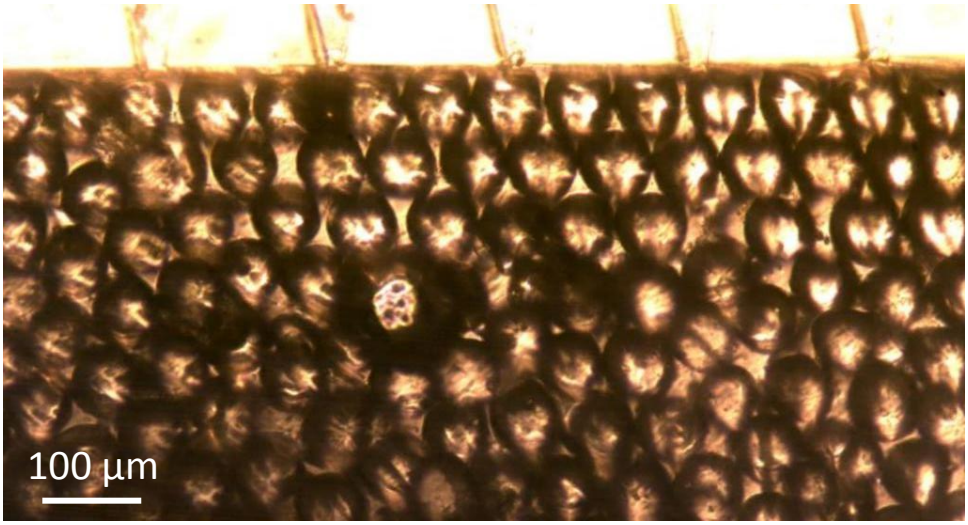

Figure 4.18: Glass spheres packing in microfluidic channel using a sonication horn

From this figure it can be seen that the packing is successful using the sonication horn, and that the viewing area is sufficient. After this method was shown to work well, this same method was used to pack the alginate spheres as shown in Figure 4.19.

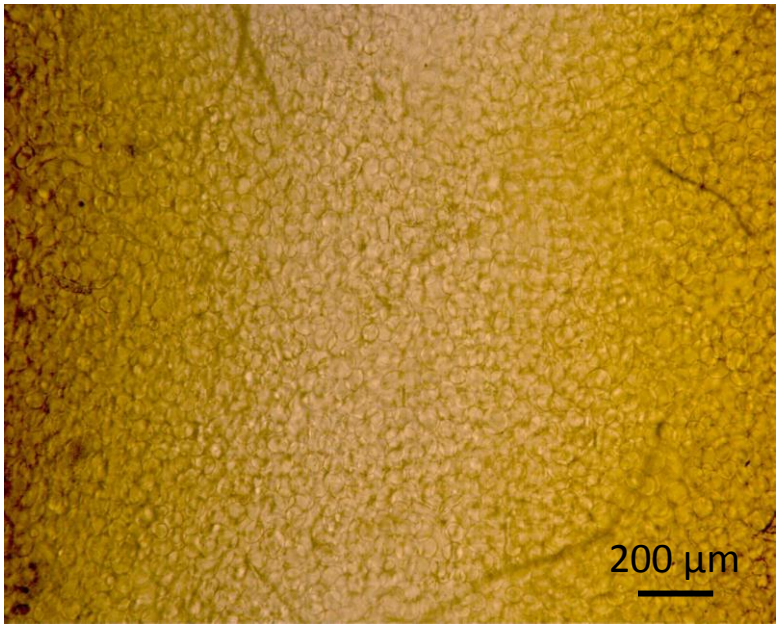

Figure 4.19: Packed alginate spheres in a microfluidic channel

This figure shows that the alginate spheres have packed the entire microchannel and that all of the spheres are approximately the same size. By looking more closely at the packed drops in Figure 4.20, more information is obtained.

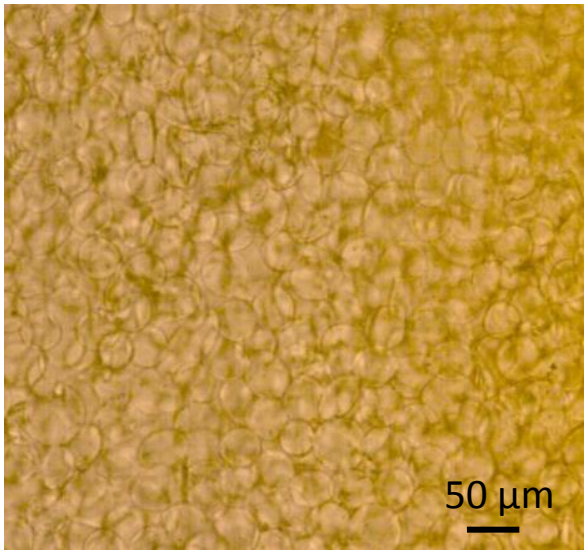

Figure 4.20: Magnified image of packed alginate spheres in a microfluidic channel

The spheres continue to hold their shape even though a large force is being exerted on each of the spheres from the packing. This shows that the method for hardening the spheres was successful.

4.4 Flowing hydrogel over spheres

After the spheres have been packed, the next step is to flow hydrogel over the spheres. Before this can occur, the oil and calcium chloride surrounding the drops must be completely removed. If the oil is not removed before the hydrogel flows over the spheres, the hydrogel will polymerize with a strange texture that is not desired for the scaffold. To rinse the spheres, Isopropyl alcohol is flowed through the spheres for five minutes. The hydrogel also does not react well to Isopropyl alcohol, so the spheres are rinsed with DI water for another five minutes. After the rinsing is complete, the UV polymerizable hydrogel is pumped through the channel at a rate of 500 μL/hr using a syringe pump. While this is occurring, the syringe, tube, and device must be covered with aluminum foil so that the hydrogel will not be polymerized prematurely. After the hydrogel covered all of the alginate drops sufficiently, the hydrogel was flowed over the drops for an additional 5 minutes to ensure total coverage.

4.5 Hydrogel Polymerization

After the hydrogel sufficiently covered all of the alginate spheres, the pump is turned off and allowed to sit for 3 minutes before the microfluidic device is placed under the UV lamp. The microfluidic device is placed under the UV lamp while still attached to the syringe and syringe pump because if not, there is no pressure to keep the microspheres packed. If too much pressure is present, the hydrogel will flow through the channel while the polymerization is occurring, and undesirable shapes and patterns form in the channel. By waiting for three minutes after the pump is turned off, the hydrogel stops flowing quickly enough to polymerize the flow patterns within the hydrogel, but still provides the pressure necessary to keep the spheres packed. To perform the UV polymerization, a short wave UV light from UVP was used which had a power of 15 Watts and a wavelength of 254 nm. The device was placed 100 mm below the light and exposed to the UV for one hour.

After the UV polymerization was complete, the polymerized hydrogel was removed from the microfluidic device by cutting the PDMS and removing the scaffold containing alginate spheres using tweezers. Figure 4.21 shows an image of the polymerized hydrogel after being removed from the microfluidics device

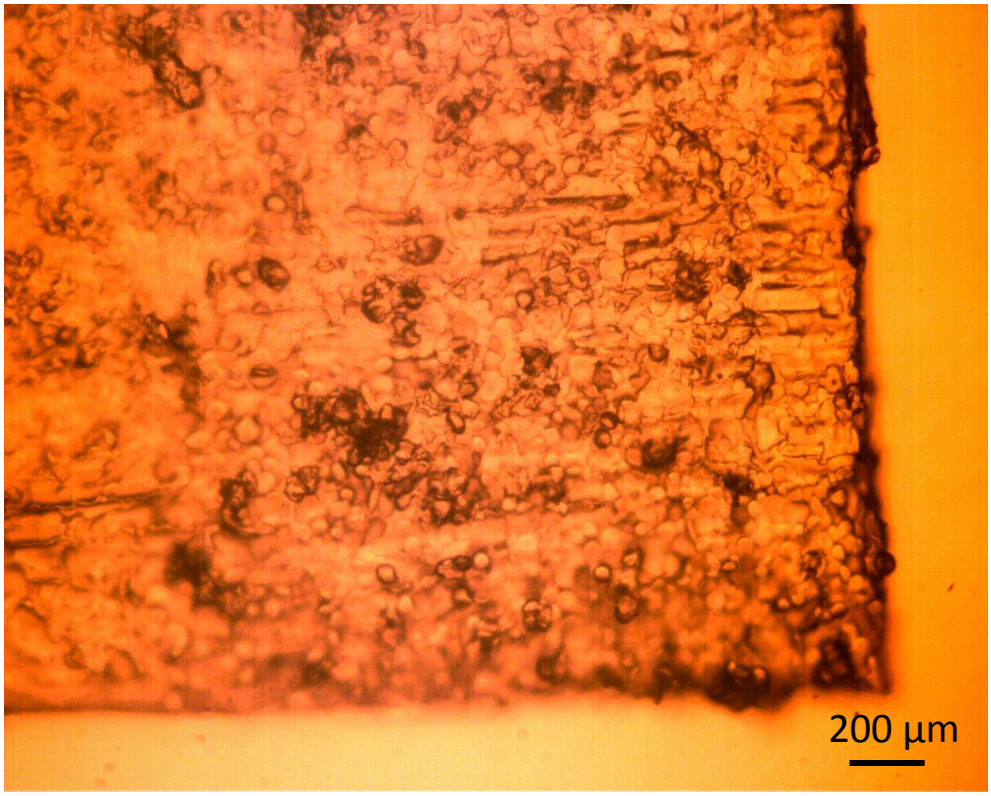

Figure 4.21: Polymerized hydrogel containing alginate microspheres after removal from the microfluidic device

The large block is formed by polymerized hydrogel, but the circular shapes within the hydrogel are the alginate spheres. Since the alginate still has a spherical shape, the alginate spheres held their shape through the polymerization of the alginate.

4.6 Rinse with EDTA

After removal from the microfluidic device, the scaffold is placed in 0.125 M EDTA purchased from Sigma to dissolve the alginate. Srivastava reported that this is possible because when the hard calcium alginate is exposed to EDTA, the Ca^{2+} crosslink are removed from the alginate gel which then solubilizes the alginate [38]. In order to get a time scale of how long it takes to dissolve the alginate in 0.125 M EDTA, a bulk test was performed with a 3 mm diameter alginate sphere. The alginate sphere was placed in a clear dish of EDTA on a Leica DMI 3000B microscope, and images were taken using a Photron Fastcam camera periodically to record the degradation of the alginate. Using this method, Figure 4.22 was produced which shows the alginate dissolving.

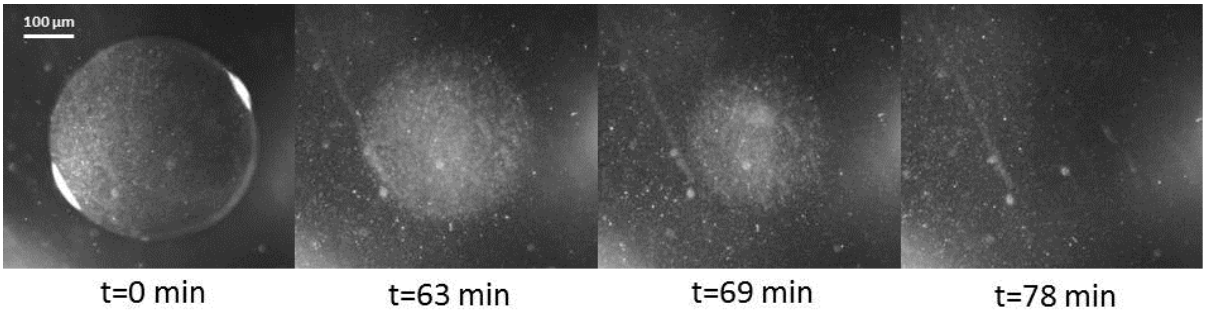

Figure 4.22: Alginate sphere dissolving in 0.125 M EDTA over time

This figure shows that the alginate dissolves in approximately 78 minutes, but it is difficult to compare actual times since the alginate drop is much bigger than the alginate drops created in the scaffold. It is also much different because the alginate drops that are encapsulated in the hydrogel will not immediately be exposed to the EDTA. Since the hydrogel forming the scaffold is not damaged by EDTA, the scaffold can be kept in the EDTA solution for multiple days without any issues. In order to be sure that all of the alginate was dissolved, the scaffold was soaked for 4 days. To make sure that the alginate that was dissolved exited the scaffold and allowed the EDTA to penetrate further into the scaffold, the EDTA solution containing the scaffold was sonicated in a Branson 2510 sonication bath for 5 times per day for 5 minutes.

Using this method the alginate drops were dissolved out of the polymerized hydrogel, creating a porous hydrogel scaffold as shown in Figure 4.23 and Figure 4.24.

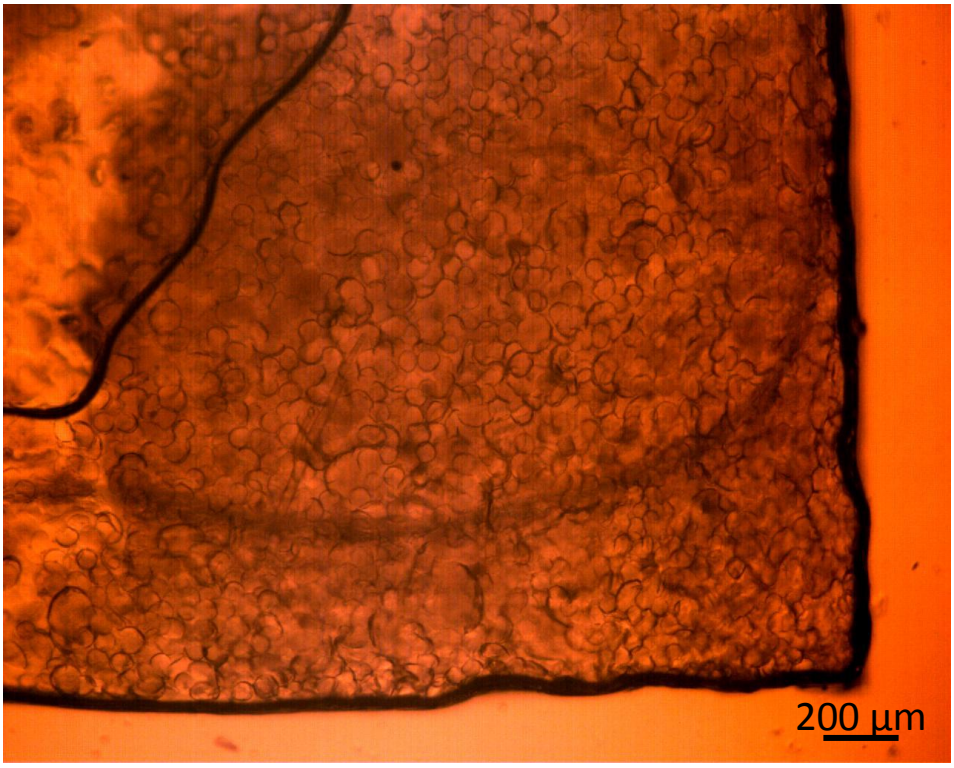

Figure 4.23: Polymerized hydrogel after alginate has been dissolved using EDTA

After dissolving out the alginate, the pores in the hydrogel are extremely easy to see. By using a greater magnification, even more detail is shown in Figure 4.24.

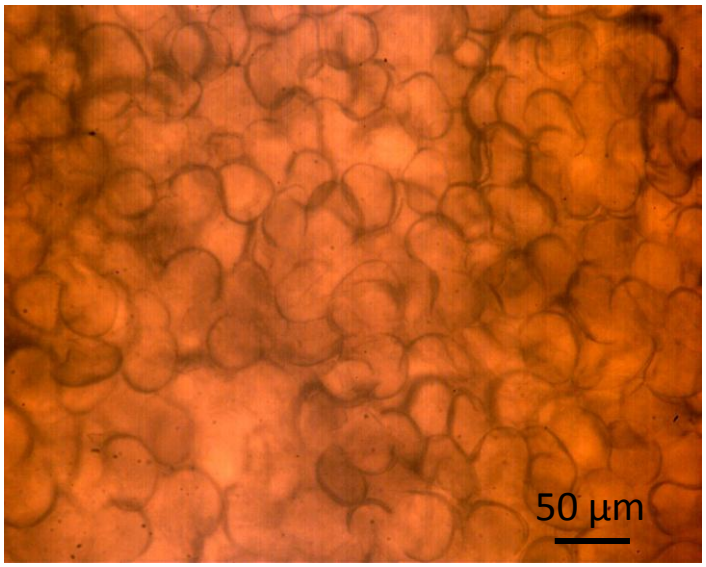

Figure 4.24: Magnified image of the polymerized hydrogel after alginate has been dissolved using EDTA

Figure 4.24 shows that the pores are packed extremely close to each other and overlap in some places. This suggests that there are interconnects that have formed in some locations. The

spherical shape is still present in the pores, and they are all approximately the same size. From this figure it is extremely difficult to tell whether the alginate has actually dissolved out of the hydrogel or not, so it is also necessary to analyze the scaffold using scanning electron microscopy (SEM) images. To prepare the scaffold for SEM imaging, the scaffold was removed from the EDTA and allowed to dry for 30 minutes. Next the scaffold was sputter coated with lead and gold so that the sample had the conductivity necessary for the imaging to take place. Figure 4.25 shows an image of the scaffold looking directly down at the cross section. The scaffold is indicated by the red arrow in the figure.

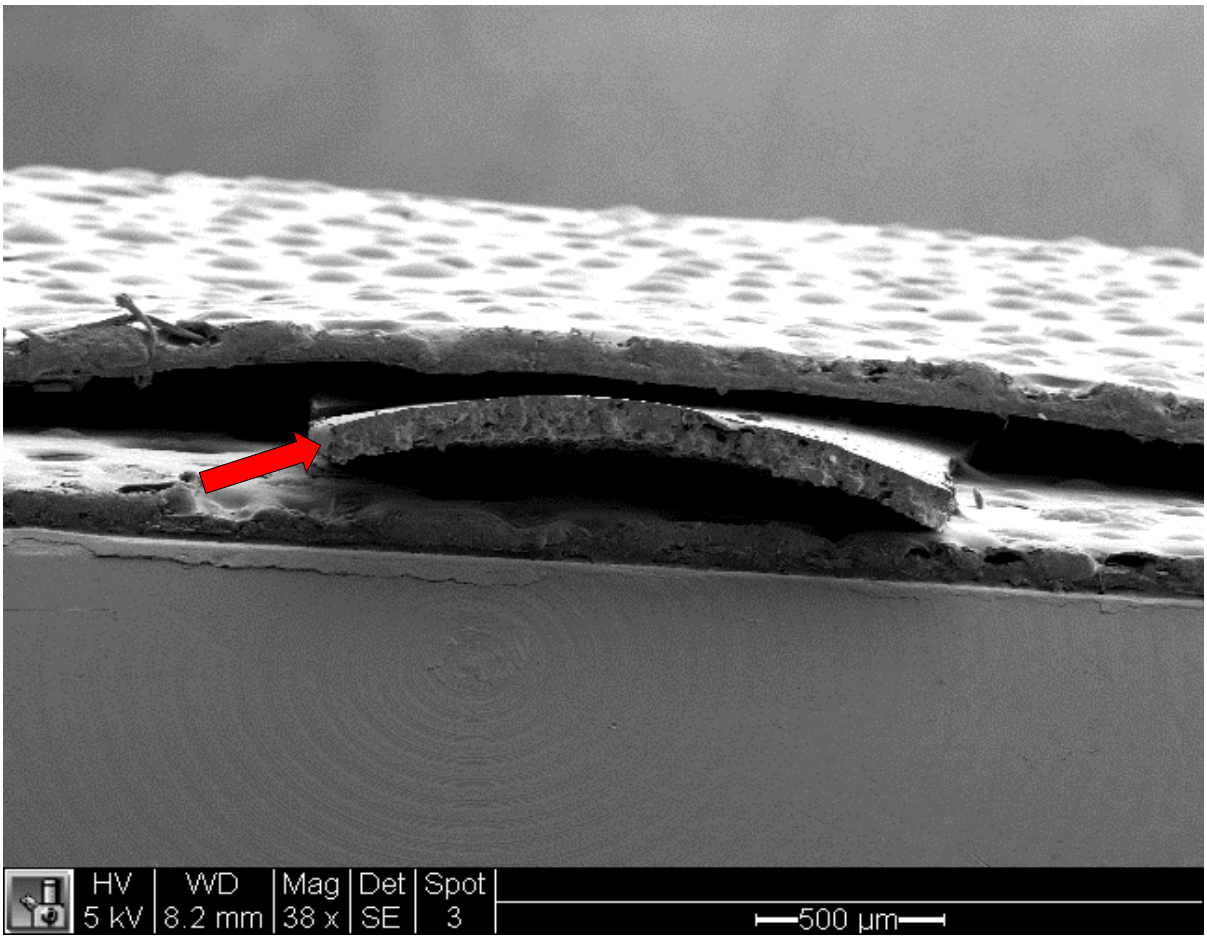

Figure 4.25: SEM image of the hydrogel scaffold showing the shape of the scaffold

It is very difficult to see much detail about the scaffold from this image, but the general size and shape of the scaffold can be seen. By magnifying the scaffold more, details about the pores can be seen as shown in Figure 4.26 and Figure 4.27.

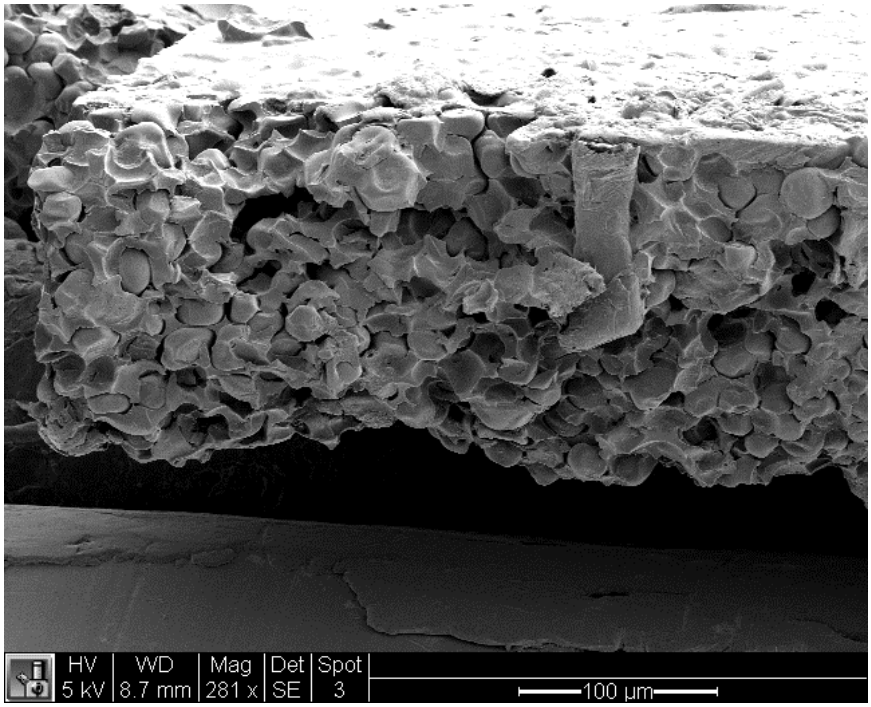

Figure 4.26: SEM image of the hydrogel scaffold

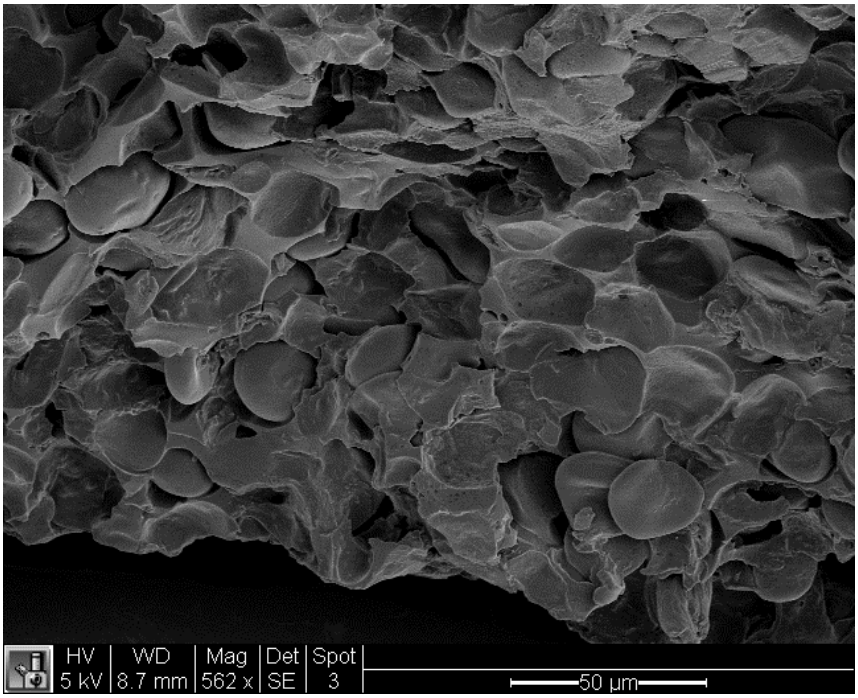

Figure 4.27: SEM image of the hydrogel scaffold showing spherical pores

These figures show that there are pores present from where the alginate spheres were once in place, and that the EDTA dissolved the alginate. It can also be confirmed that the pores are closely packed, although not in a close packed structure as desired. In these figures, however, the pores are not interconnected as desired.

Chapter 5 Future Work

Although a lot of progress has been made with creating porous hydrogel scaffolds from our work, there are still many areas where the process could be improved to produce a better scaffold.

Increasing the monodispersity of the alginate microspheres is one of the key areas to address. The microspheres that are currently being produced have more variation than is ideal for the scaffold pores. In addition to inconsistent pore sizes, polydisperse alginate spheres are also a problem because it is very difficult to have the correct ordered packing when polydispersity is present. The reason that the spheres gain polydispersity is due to alginate drops coalescing before polymerizing in the calcium chloride. To stop this from happening, the frequency of alginate drop production needs to be decreased so that the drops will not be close enough together to coalesce. In order to do this, the alginate and oil flow rates should both be decreased so that the alginate flows at approximately 20 μL/hr, and the oil at 90 μL/hr. It would also be possible to continue making the spheres the same way, but to sieve them so that only spheres within a particular size range would be used in the scaffold.

The most important characteristic to change in the current scaffold is the interconnectedness. Currently the pores of the scaffold have very limited interconnectivity for two possible reasons. The first potential cause occurs during the polymerization of the hydrogel. For the spheres to stay packed closely together, a pressure gradient needs to exist within the system. If this pressure gradient is present during the polymerization of the hydrogel, the hydrogel continues to flow while it is a liquid. Since the hydrogel changes from a liquid to a solid during this time, the shape of the polymerized hydrogel is greatly affected. An example of this is shown in Figure 5.1.

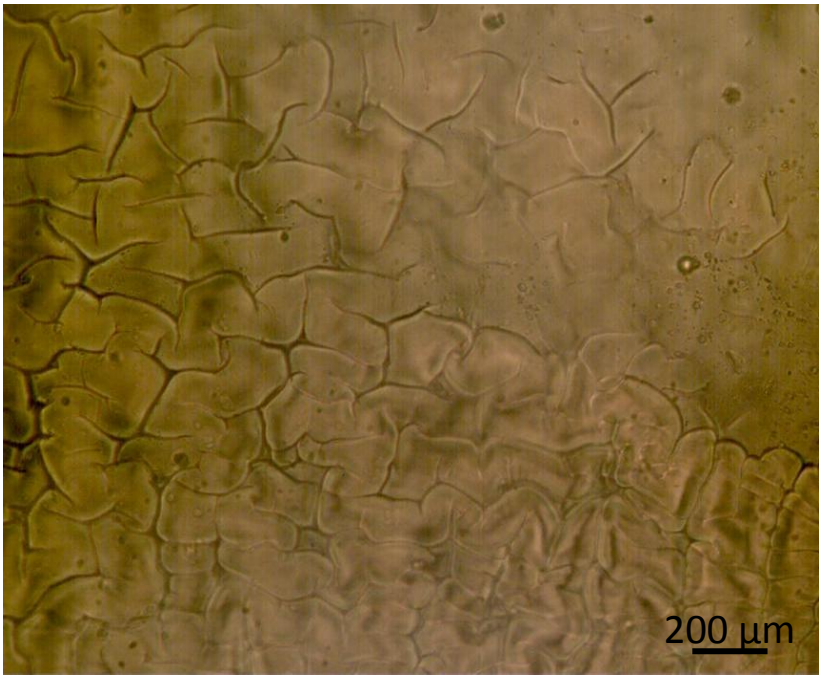

Figure 5.1: Polymerized hydrogel created during the flow of hydrogel

Figure 5.1 shows that the resulting shape of the hydrogel polymerizing under flow is not desirable. To avoid this, a pressure gradient cannot be present while the hydrogel is polymerizing. Since a pressure gradient is not present, the spheres are no longer being pressed tightly together, and the interconnects formed through the deformation of the alginate spheres is not present. To prevent this from happening, it will be necessary to link the alginate spheres together in some form so that they will not separate when pressure is no longer holding them together. The best potential method to do this is to flow EDTA through the channel so that the spheres start to soften as the alginate de-crosslinks. Calcium chloride can then be flowed through immediately after so that the crosslinking of the alginate occurs again, but this time the alginate spheres will be crosslinked together.

The limited interconnectedness may also be due to the hydrogel diffusing into the alginate spheres. A macroscale test was recently run in which 3 mm alginate microspheres were created and then packed in a syringe. The hydrogel was then flowed over the spheres and polymerized. The polymerized hydrogel containing alginate was then cut which caused some of the alginate spheres to be removed from the hydrogel. These spheres as well as the rest of the scaffold were then left in a solution of 125 mM EDTA for seven days. After seven days the alginate spheres were very soft, but they did not completely dissolve. In a previous test that used the same sized spheres and the same concentration of EDTA, the alginate that had not

been exposed to the hydrogel dissolved completely in 78 minutes. This clearly shows that being in the presence of the hydrogel drastically changes how crosslinked alginate dissolves in EDTA. The result of this is that the partially dissolved alginate spheres are present in the scaffold which does not allow the EDTA to continue to diffuse further through the scaffold and dissolve the alginate even if alginate spheres are interconnected. To stop this from happening, the diffusion of the hydrogel into the alginate needs to be stopped. The reason that the diffusion is taking place is most likely due to the fact that both the alginate and the hydrogel are primarily water based. To prevent the diffusion from happening, the hydrogel can be made by replacing the water portion of the hydrogel with ethylene glycol. Tests need to be run to verify that the hydrogel containing ethylene glycol instead of water will stop the diffusion from occurring.

Chapter 6 Conclusion

To create the porous hydrogel scaffold, many steps were performed and refined. Each of these steps is listed below with the outcome of each step.

1. Monodisperse alginate drop production- A microfluidic T-junction was used that was successfully able to create monodisperse alginate drops with a diameter of 50 μm.

2. Alginate polymerization- After trying several different methods, it was discovered that the best method for merging alginate with calcium chloride was a completely new design. Fine tuning still needs to be performed so that the polydispersity decreases, but in general the spheres are have a spherical shape and are relatively monodisperse.

3. Packing alginate spheres- The packing of the spheres was done by flowing the spheres into a microfluidic device that filtered the spheres. While the drops flowed into the device, a sonication horn was used so that the spheres settled into their thermodynamic minimum. Due to the polydispersity of the drops, the desired packing structure was not achieved with the alginate drops, but the sonication method was shown to be successful using glass spheres.

4. Flowing hydrogel - Flowing the hydrogel over the alginate spheres was done through using a syringe pump and was done very successfully.

5. UV polymerization- The polymerization of the hydrogel itself was successful, but challenges occurred when the alginate spheres did not stay packed during the polymerization. It will be necessary to implement an additional step to keep the alginate drops packed and interconnected during polymerization.

6. Rinse with EDTA- Dissolving the alginate with EDTA worked well when the alginate was not in the presence of hydrogel, but diffusion of the hydrogel into the alginate caused difficulties in dissolving the alginate. This problem should be solved by replacing the water in the hydrogel solution with ethylene glycol.

Through using this process, it was proven that creating a porous hydrogel scaffold using templating alginate microspheres is possible. However, there are still steps that need to be optimized in order to meet all of the necessary requirements for a successful scaffold.

Bibliography

1. Yang, S.F., et al., *The design of scaffolds for use in tissue engineering. Part 1. Traditional factors.* Tissue Engineering, 2001. **7**(6): p. 679-689.
2. Lee, K.Y. and D.J. Mooney, *Hydrogels for tissue engineering.* Chemical Reviews, 2001. **101**(7): p. 1869-1879.
3. Peppas, N.A., et al., *Physicochemical, foundations and structural design of hydrogels in medicine and biology.* Annual Review of Biomedical Engineering, 2000. **2**: p. 9-29.
4. Hoffman, A.S., *Hydrogels for biomedical applications.* Advanced Drug Delivery Reviews, 2002. **54**(1): p. 3-12.
5. Hua, F.J., J.D. Nam, and D.S. Lee, *Preparation of a macroporous poly(L-lactide) scaffold by liquid-liquid phase separation of a PLLA/1,4-dioxane/water ternary system in the presence of NaCl.* Macromolecular Rapid Communications, 2001. **22**(13): p. 1053-1057.
6. Marshall, A.J. and B.D. Ratner, *Quantitative characterization of sphere-templated porous biomaterials.* Aiche Journal, 2005. **51**(4): p. 1221-1232.
7. Dehghani, F. and N. Annabi, *Engineering porous scaffolds using gas-based techniques.* Current Opinion in Biotechnology, 2011. **22**(5): p. 661-666.
8. Annabi, N., et al., *Controlling the Porosity and Microarchitecture of Hydrogels for Tissue Engineering.* Tissue Engineering Part B-Reviews, 2010. **16**(4): p. 371-383.
9. Puppi, D., et al., *Polymeric materials for bone and cartilage repair.* Progress in Polymer Science, 2010. **35**(4): p. 403-440.
10. Linnes, M.P., B.D. Ratner, and C.M. Giachelli, *A fibrinogen-based precision microporous scaffold for tissue engineering.* Biomaterials, 2007. **28**(35): p. 5298-5306.
11. Barbetta, A., et al., *Polysaccharide based scaffolds obtained by freezing the external phase of gas-in-liquid foams.* Soft Matter, 2010. **6**(20): p. 5213-5224.
12. Chung, K.Y., et al., *Fabricating scaffolds by microfluidics.* Biomicrofluidics, 2009. **3**(2).
13. Drury, J.L. and D.J. Mooney, *Hydrogels for tissue engineering: scaffold design variables and applications.* Biomaterials, 2003. **24**(24): p. 4337-4351.
14. Hwang, C.M., et al., *Fabrication of three-dimensional porous cell-laden hydrogel for tissue engineering.* Biofabrication, 2010. **2**(3).
15. Malafaya, P.B., et al., *Morphology, mechanical characterization and in vivo neo-vascularization of chitosan particle aggregated scaffolds architectures.* Biomaterials, 2008. **29**(29): p. 3914-3926.
16. Marshall, A.J., et al., *Biomaterials with tightly controlled pore size that promote vascular in-growth.* Abstracts of Papers of the American Chemical Society, 2004. **228**: p. U386-U386.
17. Testouri, A., et al., *Highly Structured Foams from Chitosan Gels.* Macromolecules, 2010. **43**(14): p. 6166-6173.
18. Song, H., D.L. Chen, and R.F. Ismagilov, *Reactions in droplets in microflulidic channels.* Angewandte Chemie-International Edition, 2006. **45**(44): p. 7336-7356.
19. Tice, J.D., et al., *Formation of droplets and mixing in multiphase microfluidics at low values of the Reynolds and the capillary numbers.* Langmuir, 2003. **19**(22): p. 9127-9133.
20. Kobayashi, I., et al., *Preparation of monodisperse water-in-oil-in-water emulsions using microfluidization and straight-through microchannel emulsification.* Journal of the American Oil Chemists Society, 2005. **82**(1): p. 65-71.

21. Jakeway, S.C., A.J. de Mello, and E.L. Russell, *Miniaturized total analysis systems for biological analysis.* Fresenius Journal of Analytical Chemistry, 2000. **366**(6-7): p. 525-539.
22. Wang, H.Z., et al., *Continuous synthesis of CdSe-ZnS composite nanoparticles in a microfluidic reactor.* Chemical Communications, 2004(1): p. 48-49.
23. Christopher, G.F. and S.L. Anna, *Microfluidic methods for generating continuous droplet streams.* Journal of Physics D-Applied Physics, 2007. **40**(19): p. R319-R336.
24. Zhao, C.X. and A.P.J. Middelberg, *Two-phase microfluidic flows.* Chemical Engineering Science, 2011. **66**(7): p. 1394-1411.
25. Xu, J.H., et al., *Controllable preparation of monodisperse O/W and W/O emulsions in the same microfluidic device.* Langmuir, 2006. **22**(19): p. 7943-7946.
26. Garstecki, P., et al., *Formation of droplets and bubbles in a microfluidic T-junction - scaling and mechanism of break-up.* Lab on a Chip, 2006. **6**(3): p. 437-446.
27. Huang, K.S., T.H. Lai, and Y.C. Lin, *Manipulating the generation of Ca-alginate microspheres using microfluidic channels as a carrier of gold nanoparticles.* Lab on a Chip, 2006. **6**(7): p. 954-957.
28. Huang, K.S., et al., *Calcium alginate microcapsule generation on a microfluidic system fabricated using the optical disk process.* Journal of Micromechanics and Microengineering, 2007. **17**(8): p. 1428-1434.
29. Liu, K., et al., *Shape-controlled production of biodegradable calcium alginate gel microparticles using a novel microfluidic device.* Langmuir, 2006. **22**(22): p. 9453-9457.
30. Jin, B.J., et al., *Droplet merging in a straight microchannel using droplet size or viscosity difference.* Journal of Micromechanics and Microengineering, 2010. **20**(3).
31. Park, S.H. and Y.N. Xia, *Macroporous membranes with highly ordered and three-dimensionally interconnected spherical pores.* Advanced Materials, 1998. **10**(13): p. 1045-+.
32. Li, C.X., et al., *Experimental study on the packing of uniform spheres under three-dimensional vibration.* Powder Technology, 2011. **208**(3): p. 617-622.
33. Everett, D.H., *BASIC PRINCIPLES OF COLLOID SCIENCE*. Everett, D. H. Basic Principles of Colloid Science. Xv+243p. Royal Society of Chemistry: London, England, Uk. Illus. Paper1988.
34. Grier, D.G., *From dynamics to devices: Directed self-assembly of colloidal materials.* Mrs Bulletin, 1998. **23**(10): p. 21-21.
35. Nisisako, T., T. Torii, and T. Higuchi, *Droplet formation in a microchannel network.* Lab on a Chip, 2002. **2**(1): p. 24-26.
36. van der Graaf, S., et al., *Droplet formation in a T-shaped microchannel junction: A model system for membrane emulsification.* Colloids and Surfaces a-Physicochemical and Engineering Aspects, 2005. **266**(1-3): p. 106-116.
37. Xu, J.H., et al., *Preparation of highly monodisperse droplet in a T-junction microfluidic device.* Aiche Journal, 2006. **52**(9): p. 3005-3010.
38. Srivastava, R., et al., *Stabilization of glucose oxidase in alginate microspheres with photoreactive diazoresin nanofilm coatings.* Biotechnology and Bioengineering, 2005. **91**(1): p. 124-131.